ORGANOMETALLICS

Article

Cite This: *Organometallics* 2018, 37, 3286–3297

pubs.acs.org/Organometallics

Structure–Function Relationship in Ester Hydrogenation Catalyzed by Ruthenium CNN-Pincer Complexes

Linh Le, Jiachen Liu, Tianyi He, Daniel Kim, Eric J. Lindley, Tia N. Cervarich, Jack C. Malek, John Pham, Matthew R. Buck, and Anthony R. Chianese*

Department of Chemistry, Colgate University, 13 Oak Drive, Hamilton, New York 13346, United States

Supporting Information

ABSTRACT: A series of six pincer–ruthenium complexes has been synthesized and applied in the catalytic hydrogenation of esters. The ruthenium complexes have the formula Ru(pincer)HCl(CO), where the CNN-pincer ligands feature N-heterocyclic carbene (NHC), pyridine, and dialkylamino donor groups. Through systematic variation of the steric bulk of the NHC substituent and the amine substituents, a clear structure–function relationship emerges. The most active catalysts in this series feature the bulkiest NHC substituent employed, 2,6-diisopropylphenyl. For the dialkylamino group, catalysts substituted with isopropyl or ethyl groups were the most active, while catalysts substituted with methyl groups were significantly less active. The most active catalyst discovered catalyzes the complete hydrogenation of a range of esters at loadings of 0.05–0.2 mol %.

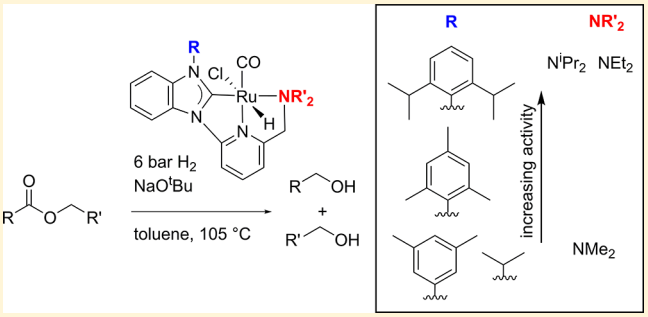

INTRODUCTION

The synthesis of alcohols by reduction of the corresponding esters is a central transformation in organic chemistry. Classical methods involving main-group hydride reagents such as $LiAlH_4$ are effective but produce stoichiometric salt byproducts that must be disposed of as waste. Reduction of esters using elemental hydrogen has historically been accomplished at the industrial scale using heterogeneous catalysts and high temperatures and pressures.[1] Homogeneous catalysts for ester hydrogenation have been known for more than 30 years,[2] but the past 10 years have seen dramatic advances in catalytic activity under moderate conditions. These advances were spurred by Milstein's 2006 report[3] of a PNN-pincer–ruthenium catalyst that operated at 115 °C and 5.3 atm hydrogen and featured a CH_2 linker arm that could be reversibly deprotonated. The catalyst was proposed to operate by a metal–ligand bifunctional mechanism wherein the Lewis acidic ruthenium atom and the basic site on the ligand cooperate in the heterolytic cleavage of H_2.

Since this seminal report, many new catalysts have been reported, which have often been designed with the bifunctional mechanism in mind. A survey of the literature revealed 20 reports[2d,4] of ester hydrogenation catalysts that give alcohols from a range of substrates in high yield with at least 1000 turnovers at full substrate conversion, seven[4a,d,g,l,n−p] of which give at least 10 000 turnovers. All of these highly active catalysts feature a transition metal supported by a multidentate ligand with a Brønsted acidic site, as motivated by Milstein's proposed cooperative mechanism.

N-Heterocyclic carbenes (NHCs)[5] are now well-established as strongly donating ligands that are capable of supporting robust and highly active catalysts for a wide variety of transformations.[6] Several multidentate ligands incorporating NHC fragments have been reported in the context of ruthenium-catalyzed ester hydrogenation or the reverse reaction,[4b,f,i,7] and Pidko's CNC-pincer–ruthenium catalysts are among the best known for this transformation in terms of turnover number and catalytic rate.[4l] We recently reported the synthesis of two CNN-pincer–ruthenium complexes (**Ru-Mes-Et** and **Ru-Mes-Me**; Chart 1) along with an initial study of their application as catalysts for ester hydrogenation.[8] In the published work, we observed that a subtle modification of the catalyst structure—changing a NMe_2 group to a NEt_2 group—resulted in a dramatic increase in catalytic activity, giving up to 980 turnovers for the hydrogenation of benzyl benzoate. Following this discovery, we embarked on a more comprehensive study of the effect of the ligand structure on the catalytic activity. Herein we report the synthesis of six new ruthenium complexes in this series (Chart 1) and a study of their comparative capabilities as ester hydrogenation catalysts. This work provided a clear picture of the effects of substituent steric bulk on the catalytic activity and resulted in the discovery of a substantially improved catalyst for ester hydrogenation.

Received: July 6, 2018
Published: September 17, 2018

DOI: 10.1021/acs.organomet.8b00470
Organometallics 2018, 37, 3286–3297

Chart 1. Ruthenium Complexes Studied in This Work

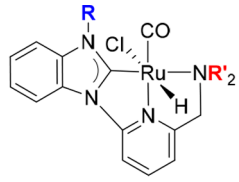

Complex	R	R'
Ru-dipp-^{i}Pr	2,6-diisopropylphenyl	^{i}Pr
Ru-dipp-Et	2,6-diisopropylphenyl	Et
Ru-dipp-Me	2,6-diisopropylphenyl	Me
Ru-Mes-^{i}Pr	mesityl	^{i}Pr
Ru-Mes-Et[a]	mesityl	Et
Ru-Mes-Me[a]	mesityl	Me
Ru-Xyl-Et	3,5-dimethylphenyl	Et
Ru-^{i}Pr-Et	isopropyl	Et

[a]Synthesis previously reported.[8]

RESULTS AND DISCUSSION

Ligand Synthesis and Metalation. We previously reported the synthesis of the ruthenium complexes **Ru-Mes-Et** and **Ru-Mes-Me** and their associated CNN-pincer ligands.[8] Six new ligands were synthesized for this work. Ligands with aromatic N-substituents on the benzimidazole ring were synthesized by analogy to our previously published route, as shown in Schemes 1−3. The new pyridyl bromide precursor **1-^{i}Pr** was synthesized by reductive amination of the aldehyde with diisopropylamine (Scheme 1). The new 1,2-diamine precursor **2-Xyl** was synthesized using a Buchwald−Hartwig coupling (Scheme 2).

Scheme 1. Reductive Amination

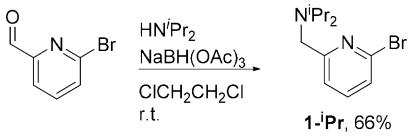

Scheme 2. Pd-Catalyzed Amination

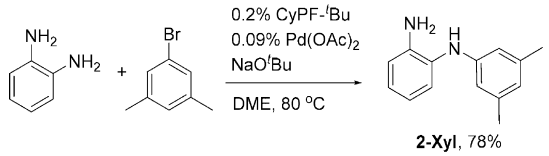

The diamines **2-dipp**, **2-Mes**, and **2-Xyl** were then coupled with **1-Me**, **1-Et**, or **1-^{i}Pr** to yield **3-dipp-^{i}Pr**, **3-dipp-Et**, **3-dipp-Me**, **3-Mes-^{i}Pr**, and **3-Xyl-Et**. These compounds were converted to the corresponding tricationic benzimidazolium salts **4-dipp-^{i}Pr**, **4-dipp-Et**, **4-dipp-Me**, **4-Mes-^{i}Pr**, and **4-Xyl-Et** using triethyl orthoformate and hydrochloric acid (Scheme 3). Our previously reported method for cyclization to obtain the benzimidazolium salts **4-Mes-Et** and **4-Mes-Me** was unpredictable, as we would often observe only partial conversion even with large excesses of triethyl orthoformate and hydrochloric acid. This may be due to the volatility of HCl combined with the very weak basicity of diarylamines. We found that when a solution of aqueous HCl in triethyl orthoformate was added dropwise to a heated solution of the

Scheme 3. Synthesis of Benzimidazolium Salts

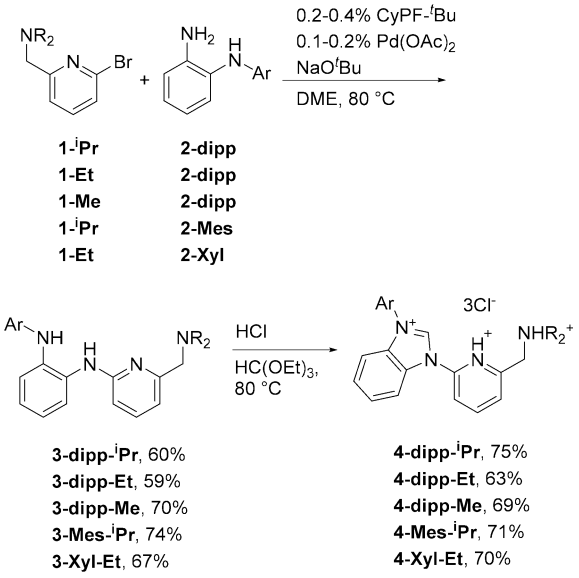

amine precursor **3** in triethyl orthoformate, the benzimidazolium salt **4** was typically formed cleanly within minutes. If reactant still remained, adding an additional quantity of HCl was effective in driving the reaction to completion.

The ligand **4-^{i}Pr-Et** was synthesized by a different path (Scheme 4). Compound **5-Et** was prepared through a copper-

Scheme 4. Synthesis of 4-^{i}Pr-Et

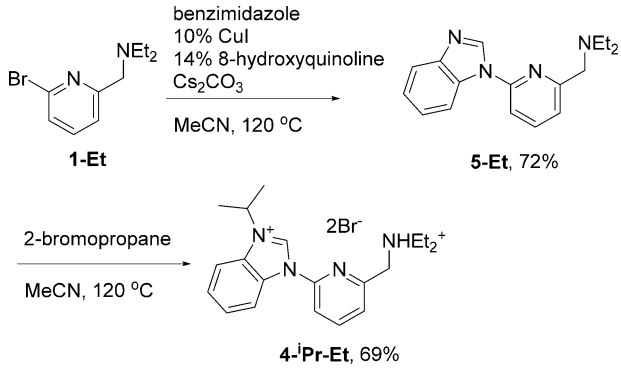

catalyzed arylation of benzimidazole with **1-Et**, by analogy to a known reaction.[9] The benzimidazole nitrogen was then alkylated using an excess of 2-bromopropane to give the ligand **4-^{i}Pr-Et** as the bromide salt, which was isolated as the dihydrobromide after chromatography.

In our previously published article,[8] we reported the synthesis of complexes **Ru-Mes-Et** and **Ru-Mes-Me**, shown in Chart 1, using transmetalation reactions between RuHCl(CO)(PPh$_3$)$_3$ and the Ag−NHC complexes,[10] which were prepared by reactions of the benzimidazolium precursors with Ag$_2$O. Though the published sequence of collection of the crude precipitate from THF followed by air-free chromatography on neutral alumina and recrystallization from CH$_2$Cl$_2$/toluene/pentane proved to be successful for these complexes, the method was not successful when applied to the complexes **Ru-Xyl-Et** and **Ru-^{i}Pr-Et**, as the crude reaction mixtures showed a sluggish reaction with concomitant formation of unidentified side products. The issue may stem from the

DOI: 10.1021/acs.organomet.8b00470
Organometallics 2018, 37, 3286−3297

incomplete dissociation of the PPh_3 ligands on the Ru precursor, leading to low yields of the target complexes.

To counter this problem, excess silver chloride was added to the transmetalation reaction mixture along with the starting materials in order to act as a "phosphine sponge" (Scheme 5).

Scheme 5. Synthesis of Ruthenium Complexes

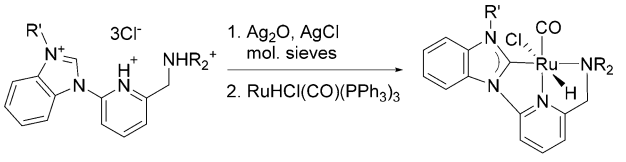

4-dipp-^{i}Pr
4-dipp-Et
4-dipp-Me
4-Mes-^{i}Pr
4-Xyl-Et
4-^{i}Pr-Et[a]

Ru-dipp-^{i}Pr, 47%
Ru-dipp-Et, 56%
Ru-dipp-Me, 50%
Ru-Mes-^{i}Pr, 52%
Ru-Xyl-Et, 38%
Ru-^{i}Pr-Et, 16%

[a]Ligand precursor formulated as the dihydrobromide salt

The AgCl reacts with PPh_3 to quantitatively form the known cluster $Ag_4Cl_4(PPh_3)_4$,[11] which we previously observed and confirmed by X-ray crystallography.[8] This in turn promotes the dissociation of PPh_3 from $RuHCl(CO)(PPh_3)_3$ to be replaced by the CNN-pincer. In addition, all of the transmetalation reactions proceed at a higher rate in the presence of excess AgCl. We were not able to obtain **Ru-Xyl-Et** or **Ru-^{i}Pr-Et** in analytically pure form, as these compounds were strongly retained on silica gel and consistently coeluted with minor impurities, including $Ag_4Cl_4(PPh_3)_4$, which were not removed by bulk recrystallization. As these complexes were only moderately active catalysts for ester hydrogenation (vide infra), we did not pursue their purification further.

Structural Analysis. The six new ruthenium complexes were characterized by X-ray crystallography. These complexes, along with the previously reported **Ru-Mes-Me** and **Ru-Mes-Et**, are closely analogous structurally. Figure 1 shows the structure of **Ru-dipp-Et**; ORTEP diagrams for the remaining five complexes are included in the Supporting Information. All of the complexes possess an octahedral structure in which the chloride ligand is trans to the hydride. These compounds have similar bond lengths and bond angles. One notable exception is that the Ru(1)−N(21) bond is slightly longer in complexes with isopropylamine substituents (2.346−2.355 Å) than in complexes with methyl- or ethylamine substituents (2.245−2.315 Å). The arrangement of ligands around the metal center—the hydride and halide ligands mutually trans and the carbonyl ligand in-plane with the pincer ligand—is consistent with that in all previously reported ruthenium complexes of the formula Ru(pincer)HCl(CO).[4g,12]

The geometry observed in the solid state is retained in solution, on the basis of data from the NMR spectra. For **Ru-^{i}Pr-Et**, nuclear Overhauser spectroscopy (NOESY) showed the expected correlation between the hydride and the ^{i}Pr substituent on the benzimidazole ring. Similarly for the remaining species bearing aromatic substituents, the same correlation between the hydride and the ortho substituent of the ring was observed. For instance, when the NHC substituent is mesityl, the NOESY cross-peak appears between the ruthenium hydride and the ortho CH_3 group on the mesityl ring. When the NHC substituent is 3,5-xylyl, a cross-peak appears between the hydride and the ortho hydrogen on the xylyl ring.

Ester Hydrogenation: Catalyst Comparison. The six new ruthenium complexes were tested for ester hydrogenation to systematically compare their activities with each other and those of the previously published complexes **Ru-Mes-Me** and **Ru-Mes-Et**. The reactions were carried out under 6 bar H_2 and employed catalytic amounts of NaO^{t}Bu at 105 °C in toluene (Scheme 6).

Scheme 6. Conditions for Systematic Catalyst Comparison

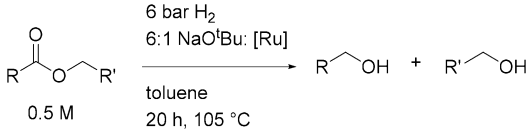

We employed three model substrates, ethyl benzoate (Figure 2), hexyl hexanoate (Figure 3), and methyl benzoate (Figure 4), in order to compare the activities of the eight catalysts and to determine whether the variation in activity is consistent for different substrates. In each reaction, the substrate concen-

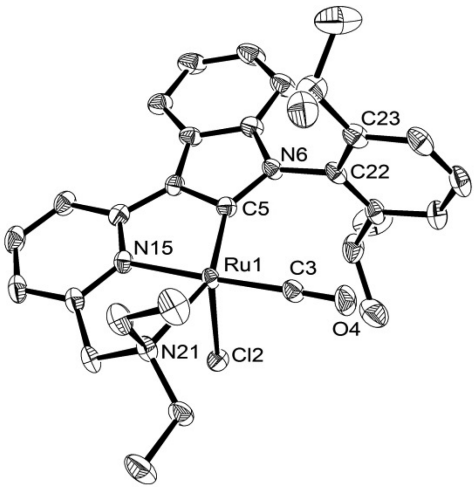

Figure 1. ORTEP diagram of **Ru-dipp-Et**, showing 50% probability ellipsoids. Hydrogen atoms have been omitted for clarity.

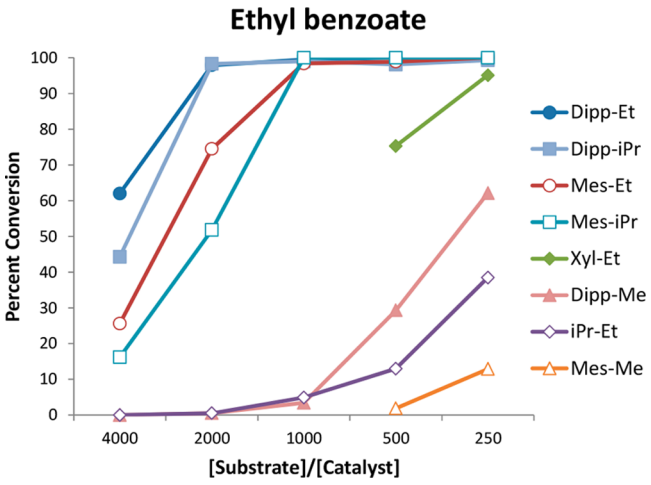

Figure 2. Comparison of ruthenium catalysts for hydrogenation of ethyl benzoate under the conditions in Scheme 6.

DOI: 10.1021/acs.organomet.8b00470
Organometallics 2018, 37, 3286−3297

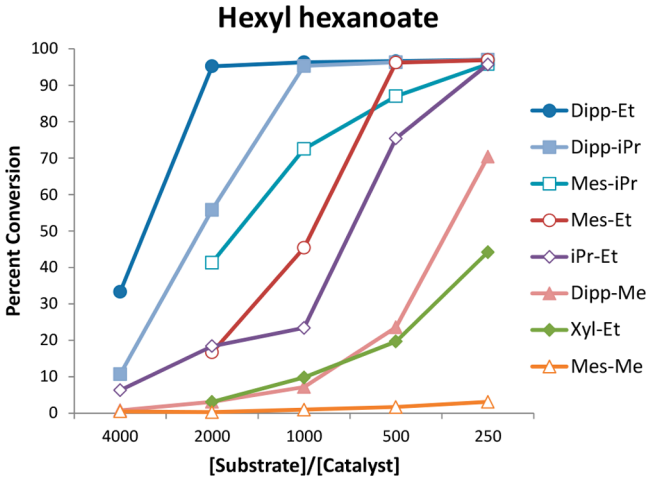

Figure 3. Comparison of ruthenium catalysts for hydrogenation of hexyl hexanoate under the conditions in Scheme 6.

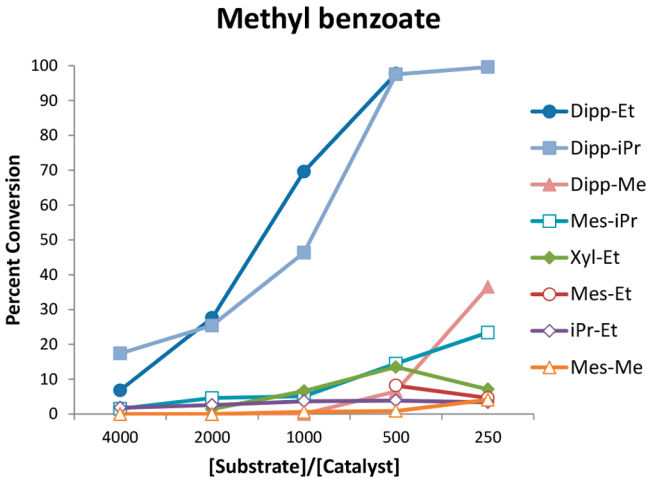

Figure 4. Comparison of ruthenium catalysts for hydrogenation of methyl benzoate under the conditions in Scheme 6.

tration and the [base]:[Ru] ratio were maintained at 0.5 M and 6:1, respectively, while the [substrate]:[Ru] ratio was varied from 4000:1 to 250:1.

As shown in Figures 2–4, two principal observations emerge from the data. First, changing the steric bulk of the substituent on the NHC substituent dramatically alters the ester hydrogenation activity of the complex. It is clear that the most active catalysts for all three substrates contain the bulky dipp substituent, for which full conversion is attained with a substrate:catalyst ratio as high as 2000:1. With the smaller mesityl substituent, the catalysts are less active. With the even smaller 3,5-xylyl and isopropyl substituents, the activity is further diminished for all three substrates.

Varying the substituent on the amine arm has a significant effect on the catalyst activity as well. For both the dipp- and Mes-substituted series of catalysts, the NEt_2- and N^iPr_2-substituted variants were similar in activity, while the NMe_2-substituted variant had substantially diminished activity. **Ru-dipp-Me** gave a maximum conversion of 70%, and **Ru-Mes-Me** gave a maximum conversion of 13%, both at the highest catalyst loading tested. This dramatic effect for a relatively minor steric modification may potentially be explained by differential energetics of substrate/product binding but also raises the possibility of a mechanism involving dechelation of the amine arm,[13] which would be expected to be less costly for bulkier amine substituents.

Importantly, two of our new catalysts show activity toward methyl benzoate, which was not effectively hydrogenated under these conditions by our prototype catalysts **Ru-Mes-Me** and **Ru-Mes-Et**.[8] As indicated in Figure 4, two complexes containing the dipp substituent on the benzimidazole side, **Ru-dipp-iPr** and **Ru-dipp-Et**, gave complete hydrogenation of methyl benzoate at a 500:1 substrate to catalyst ratio.

Ester Hydrogenation: Substrate Scope. With the identification of **Ru-dipp-^{i}Pr** and **Ru-dipp-Et** as the most active catalysts, we chose **Ru-dipp-Et** for experiments with a wider range of substrates since it was slightly more active than **Ru-dipp-^{i}Pr** in our initial exploration and is easier to synthesize. A range of catalyst loadings were employed, and Table 1 shows the lowest loadings that gave full or nearly full conversion. The catalyst is effective in the hydrogenation of various aromatic and aliphatic esters, such as methyl, ethyl and benzyl esters. Similarly to our published results, phthalide requires a pressure of 30 bar for nearly full conversion, likely because of thermodynamic effects.[4f,l,14] All of the substrates were fully or nearly fully hydrogenated at a catalyst loading of 0.2% ([substrate]:[catalyst] = 500:1), a 4-fold increase from our previous study using **Ru-Mes-Et** and the same esters. It is also noteworthy that apart from methyl benzoate, the two

Table 1. Substrate Scope for Ester Hydrogenation Catalyzed by Ru-dipp-Et

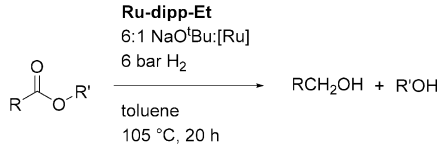

Substrate	Substrate:[Ru]	Yield[a]
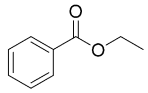	2000:1	98% (92%)
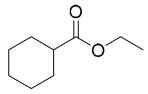	500:1	99%
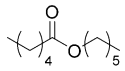	2000:1	95%
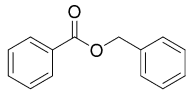	1000:1	98% (89%)
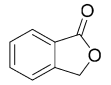	1000:1 (30 bar H_2)	82% (72%)
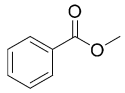	500:1	98%
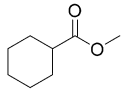	1000:1 (30 bar H_2)	>99%
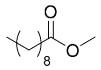	2000:1 (30 bar H_2)	>99%

[a]Isolated yields at 1.0 mmol scale are given in parentheses.

DOI: 10.1021/acs.organomet.8b00470
Organometallics 2018, 37, 3286–3297

other methyl esters, methyl cyclohexanecarboxylate and methyl decanoate, required a hydrogen pressure of 30 bar for full conversion. When the experiments were conducted at 6 bar, we observed incomplete conversion and substantial transesterification[15] to produce species such as decyl decanoate (from methyl decanoate).

Thus, through a systematic examination of the relationship between ligand structure and catalytic activity, we have identified an improved hydrogenation catalyst for a wide range of ester substrates that gives high turnover numbers at low or moderate pressures. Although this represents a substantial improvement, the turnover numbers observed for **Ru-dipp-Et** are still lower than those measured for the best catalysts in the literature[4a,d,g,l,n−p]

Reduction of Additional Functional Groups. An important parameter in the development of new catalysts is chemoselectivity for the functional group of interest. To provide an initial assessment of the broader scope of hydrogenation activity for **Ru-dipp-Et**, we attempted the hydrogenation of the range of substrates shown in Table 2. The reaction conditions employed were identical to those developed for ester hydrogenation, except that we only conducted reactions with a substrate:ruthenium ratio of 500:1.

Table 2. Hydrogenation of Polar and Nonpolar Substrates Catalyzed by Ru-dipp-Et

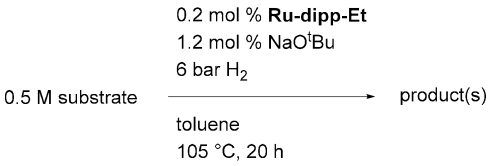

Substrate	Product(s)	Yield
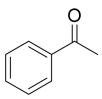	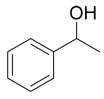	96%
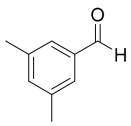	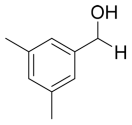	>99%
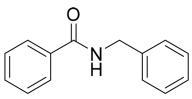	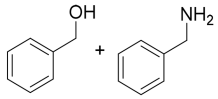	36%, 34%
	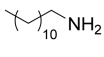	12%
		99%
		96%

Under these conditions, we observed complete, clean hydrogenation of acetophenone and 3,5-dimethylbenzaldehyde. This result is consistent with those for related ruthenium[4g,16] and iridium[4h] catalysts for ester hydrogenation and is unsurprising as these functional groups are generally more reactive toward reduction. The hydrogenation of amides[12d,g,14d,16,17] and nitriles[18] is more challenging, and under these unoptimized conditions, we observed low conversion of *N*-benzylbenzamide and dodecanitrile to the hydrogenated products. In both cases the reactions were very clean, with only the products shown and unreacted starting materials observed by NMR and GC. This suggests that with further experimentation, it may be possible to develop effective conditions for the hydrogenation of amides and/or nitriles with our catalyst system. The reactivity of catalysts for ester hydrogenation toward nonpolar substrates such as alkenes and alkynes is varied, although some catalysts have been shown to be highly specific for ester hydrogenation in the presence of both terminal and internal (nonconjugated) alkenes.[4n,19] We are aware of one example of an ester hydrogenation catalyst that is tolerant of internal alkynes, reported by Clarke and coworkers.[19a] Under our optimized conditions for ester hydrogenation, **Ru-dipp-Et** catalyzed the complete hydrogenation of both 1-dodecene and 1-dodecyne to *n*-dodecane, indicating that it is not selective for C═O bonds over C═C bonds.

CONCLUSION

Six new ruthenium−CNN-pincer complexes (**Ru-dipp-^{i}Pr**, **Ru-dipp-Et**, **Ru-dipp-Me**, **Ru-Mes-^{i}Pr**, **Ru-Xyl-Et**, and **Ru-^{i}Pr-Et**) were synthesized and employed as catalysts for ester hydrogenation to study the relationship between the steric bulk of ligand substituents and the catalytic activity. Greater steric bulk of the NHC substituent was clearly associated with increased activity. On the amine arm, ethyl and isopropyl substituents were nearly equivalent, but drastically reduced catalyst activity was observed with methyl substituents. The most active catalyst, **Ru-dipp-Et**, demonstrated an improved substrate scope toward a range of aliphatic and aromatic esters compared with our previously reported complex **Ru-Mes-Et**. Current work is directed at developing an understanding of the reaction mechanism as well as the origin of the structure−function relationships described above.

EXPERIMENTAL SECTION

General Methods. Unless stated otherwise, all of the reactions were carried out either on a Schlenk line under argon or in an argon-filled MBraun Labmaster 130 glovebox. Solvents were purified by sparging with argon and passage through columns of activated alumina using an MBraun solvent purification system. All of the reagents and materials were commercially available and used as received, unless otherwise noted. For the ruthenium precursor $RuHCl(CO)(PPh_3)_3$, both commercially purchased samples (Alfa Aesar) and synthesized material, prepared according to a literature method,[20] were used. Flash chromatography employing solvent gradients was performed using a Teledyne Isco Combiflash RF system. NMR spectra were recorded at room temperature on a Bruker spectrometer (400 MHz for ^{1}H NMR and 100 MHz for ^{13}C NMR) and referenced to the residual solvent resonance (δ in parts per million, J in hertz). Elemental analyses were performed by Robertson Microlit (Madison, NJ). High-resolution mass spectroscopic analysis was performed at the University of Illinois Mass Spectroscopic Laboratory (Urbana, IL). Detailed NMR assignments for the newly reported ruthenium complexes are given in the Supporting Information. Compound **2-dipp** was synthesized as previously described.[21]

Synthesis of 1-^{i}Pr. A Schlenk flask was flame-dried, and 6-bromopyridine-2-carboxaldehyde (3.42 g, 18.4 mmol) was added. The flask was purged and filled with argon. Dichloroethane (70 mL) and diisopropylamine (12.9 mL, 92.2 mmol) were added, and the mixture was stirred for 5 min. Then sodium triacetoxyborohydride (5.47 g, 18.4 mmol) was added, and the mixture was stirred for 1.5 h. The flask was opened, and 70 mL of 10% aqueous sodium hydroxide was added. The mixture was stirred for 10 min and then poured into a separatory funnel along with 150 mL of diethyl ether. The aqueous layer was removed, and the organic layer was washed three times with 40 mL of 10% aqueous sodium hydroxide. The organic layer was then

DOI: 10.1021/acs.organomet.8b00470
Organometallics 2018, 37, 3286−3297

collected, dried over $MgSO_4$, filtered, and concentrated. The crude residue was purified by flash chromatography on silica gel using a gradient of 0−30% isopropanol in hexanes. After evaporation of the solvent, the product was obtained as a yellow solid. Yield: 3.28 g, 66%. ^{1}H NMR ($CDCl_3$): δ 7.59 (d, $^3J_{HH}$ = 7.6 Hz, 1H), 7.44 (t, $^3J_{HH}$ = 7.7 Hz, 1H), 7.23 (d, $^3J_{HH}$ = 7.7 Hz, 1H), 3.73 (s, 2H), 3.06−2.91 (hept, $^3J_{HH}$ = 6.6 Hz, 2H), 0.97 (d, $^3J_{HH}$ = 6.6 Hz, 12H). ^{13}C{^{1}H} NMR: δ 166.51, 140.74, 138.68, 125.26, 120.58, 51.15, 49.16, 20.87. HRMS (EI+): calcd for $C_{12}H_{19}N_2Br$, 270.0732; found, 270.0725.

Synthesis of 2-Xyl. $Pd(OAc)_2$ (2.8 mg, 0.013 mmol), (*R*)-(−)-1-[(*S*)-2-(dicyclohexylphosphino)ferrocenyl]ethyl-di-*tert*-butylphosphine (CyPF-tBu) (14.1 mg, 0.025 mmol), a stir bar, and 1,2-dimethoxyethane (10 mL) were added to a 40 mL oven-dried vial in the glovebox. After the mixture became homogeneous, 1-bromo-3,5-dimethylbenzene (1.73 mL, 2.35 g, 12.7 mmol), *o*-phenylenediamine (2.75 g, 25.4 mmol), and NaO^{t}Bu (1.83 g, 19.1 mmol) were added. The vial was capped and heated at 80 °C overnight while stirring. The vial was opened, and the mixture was filtered through a plug of silica with 100 mL of ethyl acetate. The solvent was evaporated, and the residue was purified by flash chromatography on silica gel using a gradient of 0 to 30% ethyl acetate in hexanes. Yield: 2.26 g, 78%. ^{1}H NMR ($CDCl_3$): δ 7.16 (d, $^3J_{HH}$ = 7.6 Hz, 1H), 7.07 (t, $^3J_{HH}$ = 7.5 Hz, 1H), 6.88−6.77 (m, 2H), 6.54 (s, 1H), 6.42 (s, 2H), 5.13 (br s, 1H), 3.79 (br s, 2H), 2.29 (s, 6H). ^{13}C{^{1}H} NMR: δ 145.47, 142.07, 139.14, 128.82, 125.63, 125.08, 121.33, 119.16, 116.18, 113.11, 21.52. HRMS (EI+): calcd for $C_{14}H_{16}N_2$, 212.1314; found, 212.1310.

Synthesis of 3-dipp-^{i}Pr. $Pd(OAc)_2$ (2.8 mg, 0.012 mmol), CyPF-tBu (13.8 mg, 0.025 mmol), a stir bar, and 1,2-dimethoxyethane (10 mL) were added to a 40 mL oven-dried vial in the glovebox. After the mixture became homogeneous, **1-^{i}Pr** (1.69 g, 6.22 mmol), **2-dipp**[21] (1.67 g, 6.22 mmol), and NaO^{t}Bu (1.79 g, 18.7 mmol) were added. The vial was capped and heated at 80 °C overnight while stirring. The vial was opened, and the mixture was filtered through a plug of silica gel with 100 mL of a 1:4 mixture of methanol and ethyl acetate. The solvent was evaporated, and the residue was purified by flash chromatography on silica gel using a gradient of 0 to 20% methanol in dichloromethane. Yield: 1.71 g, 60%. NMR spectra were obtained in C_6D_6 because decomposition was sometimes observed in $CDCl_3$. Note: two ^{1}H and ^{13}C signals were seen for the four methyl groups on the 2,6-diisopropylphenyl substituent because of hindered rotation about the N−C_{aryl} bond. ^{1}H NMR (C_6D_6): δ 8.16 (br s, 1H), 7.29−7.13 (m, 6H), 7.10 (d, $^3J_{HH}$ = 7.8 Hz, 2H), 6.89 (t, $^3J_{HH}$ = 7.7 Hz, 1H), 6.63 (t, $^3J_{HH}$ = 7.5 Hz, 1H), 6.36 (d, $^3J_{HH}$ = 8.1 Hz, 2H), 5.96 (br s, 1H), 3.68 (s, 2H), 3.17 (hept, $^3J_{HH}$ = 6.8 Hz, 2H), 2.96 (hept, $^3J_{HH}$ = 6.5 Hz, 2H), 1.11 (d, $^3J_{HH}$ = 7.0 Hz, 6H), 0.96 (d, $^3J_{HH}$ = 6.4 Hz, 6H), 0.93 (d, $^3J_{HH}$ = 6.5 Hz, 12H). ^{13}C{^{1}H} NMR: δ 163.35, 158.96, 147.42, 145.79, 138.34, 135.80, 129.00, 127.93, 127.61, 126.05, 124.11, 118.28, 112.60, 112.33, 104.89, 51.88, 49.12, 28.67, 24.63, 23.24, 20.96. HRMS (EI+): calcd for $C_{30}H_{42}N_4$, 458.3409; found, 458.3401.

Synthesis of 3-dipp-Et. $Pd(OAc)_2$ (6.8 mg, 0.030 mmol), CyPF-tBu (33.4 mg, 0.060 mmol), a stir bar, and 1,2-dimethoxyethane (75 mL) were added to a 150 mL medium-pressure vessel in the glovebox. After the mixture became homogeneous, **1-Et** (3.67 g, 15.1 mmol), **2-dipp**[21] (4.05 g, 15.1 mmol), and NaO^{t}Bu (4.35 g, 45.2 mmol) were added. The vessel was capped, removed from the glovebox, and heated at 80 °C overnight while stirring. The vessel was opened, and the mixture was filtered through a plug of silica gel with 100 mL of a 1:4 mixture of methanol and ethyl acetate. The solvent was evaporated, and the residue was purified by flash chromatography on silica gel using a gradient of 0 to 20% methanol in dichloromethane. Yield: 3.82 g, 59%. Note: two ^{1}H and ^{13}C signals were seen for the four methyl groups on the 2,6-diisopropylphenyl substituent because of hindered rotation about the N−C_{aryl} bond. ^{1}H NMR ($CDCl_3$): δ 7.41 (t, $^3J_{HH}$ = 7.8 Hz, 1H), 7.30−7.18 (m, 4H), 7.00 (t, $^3J_{HH}$ = 7.8 Hz, 1H), 6.85 (d, $^3J_{HH}$ = 7.3 Hz, 1H), 6.71 (t, $^3J_{HH}$ = 7.6 Hz, 1H), 6.34 (d, $^3J_{HH}$ = 8.2 Hz, 1H), 6.23 (d, $^3J_{HH}$ = 7.5 Hz, 1H), 6.22 (br s, 1H), 5.68 (br s, 1H), 3.60 (s, 2H), 3.08 (hept, $^3J_{HH}$ = 6.8 Hz, 2H), 2.61 (q, $^3J_{HH}$ = 7.1 Hz, 4H), 1.19−0.98 (m, 18H). ^{13}C{^{1}H} NMR: δ 159.18, 157.94, 147.34, 144.91, 138.05, 134.97, 127.50 (two peaks overlapped), 127.20, 124.86, 123.75, 117.49, 113.80, 112.21, 105.04, 59.53, 47.34, 28.26, 24.50, 23.10, 11.69. HRMS (EI+): calcd for $C_{28}H_{38}N_4$, 430.3096; found, 430.3082.

Synthesis of 3-dipp-Me. $Pd(OAc)_2$ (2.9 mg, 0.013 mmol), CyPF-tBu (14.1 mg, 0.025 mmol), a stir bar, and 1,2-dimethoxyethane (70 mL) were added to a 150 mL medium-pressure vessel in the glovebox. After the mixture became homogeneous, **1-Me** (1.37 g, 6.4 mmol), **2-dipp**[21] (1.71 g, 6.4 mmol), and NaO^{t}Bu (1.84 g, 19.1 mmol) were added. The vessel was capped, removed from the glovebox, and heated at 80 °C overnight while stirring. The vessel was opened, and the mixture was filtered through a plug of silica gel with 100 mL of a 1:4 mixture of dichloromethane and methanol. The solvent was evaporated, and the residue was purified by flash chromatography on silica gel using a gradient of 0 to 30% methanol in dichloromethane. Yield: 1.79 g, 70%. Note: two ^{1}H and ^{13}C signals were seen for the four methyl groups on the 2,6-diisopropylphenyl substituent because of hindered rotation about the N−C_{aryl} bond. ^{1}H NMR (CD_2Cl_2): δ 7.48−7.38 (m, 1H), 7.30−7.18 (m, 4H), 7.05−6.93 (m, 1H), 6.87−6.76 (m, 1H), 6.71 (td, $^3J_{HH}$ = 7.5 Hz, $^4J_{HH}$ = 1.4 Hz, 1H), 6.48 (s, 1H), 6.34 (d, $^3J_{HH}$ = 8.1 Hz, 1H), 6.20 (dd, $^3J_{HH}$ = 8.1 Hz, $^4J_{HH}$ = 1.4 Hz, 1H), 5.73 (s, 1H), 3.40 (s, 2H), 3.09 (hept, *J* = 6.9 Hz, 2H), 2.25 (s, 6H), 1.08 (dd, *J* = 17.5, 5.9 Hz, 12H). ^{13}C{^{1}H} NMR (101 MHz, CD_2Cl_2): δ 158.15, 157.95, 147.38, 144.96, 138.01, 135.12, 127.52, 127.35, 127.18, 125.19, 123.73, 117.47, 113.64, 112.15, 105.19, 65.73, 45.44, 28.24, 24.24, 22.83. HRMS (ESI+): calcd for $C_{26}H_{35}N_4$ (M + H), 403.2862; found, 403.2859.

Synthesis of 3-Mes-^{i}Pr. $Pd(OAc)_2$ (2.2 mg, 0.010 mmol), CyPF-tBu (10.6 mg, 0.019 mmol), a stir bar, and 1,2-dimethoxyethane (10 mL) were added to a 20 mL oven-dried vial in the glovebox. After the mixture became homogeneous, **1-iPr** (1.30 g, 4.79 mmol), **2-Mes** (1.09 g, 4.79 mmol), and NaO^{t}Bu (691 mg, 7.19 mmol) were added. The vial was capped and heated at 80 °C overnight while stirring. The vial was then removed from the glovebox, and the mixture was filtered through a plug of silica gel with 200 mL of 20% ethanol in ethyl acetate. The solvent was evaporated, and the residue was purified by flash chromatography on silica gel using a gradient of 0 to 20% methanol in dichloromethane. Yield: 1.479 mg, 74%. ^{1}H NMR (CD_2Cl_2): δ 7.46 (t, $^3J_{HH}$ = 7.6 Hz, 1H), 7.30 (d, $^3J_{HH}$ = 7.8 Hz, 1H), 7.08 (m, 2H), 7.02 (t, $^3J_{HH}$ = 7.6 Hz, 1H), 6.92 (s, 2H), 6.76 (t, $^3J_{HH}$ = 7.6 Hz, 1H), 6.34 (d, $^3J_{HH}$ = 8.1 Hz, 1H), 6.23 (d, *J* = 8.1 Hz, 1H), 5.74 (s, 1H), 3.60 (s, 2H), 3.06 (hept, $^3J_{HH}$ = 6.5 Hz, 2H), 2.31 (s, 3H), 2.10 (s, 6H), 1.02 (d, *J* = 6.5 Hz, 12H). ^{13}C{^{1}H} NMR: δ 162.89, 157.42, 143.09, 137.97, 135.67, 135.37, 135.25, 129.05, 127.11, 126.93, 126.20, 117.74, 112.23, 112.13, 104.69, 51.20, 48.80, 20.62, 20.53, 17.89. HRMS (EI+): calcd for $C_{27}H_{36}N_4$, 416.2940; found, 416.2946.

Synthesis of 3-Xyl-Et. $Pd(OAc)_2$ (2.3 mg, 0.010 mmol), CyPF-tBu (11.3 mg, 0.020 mmol), a stir bar, and 1,2-dimethoxyethane (20 mL) were added to a 40 mL oven-dried vial in the glovebox. After the mixture became homogeneous, **1-Et** (2.47 g, 10.1 mmol), **2-Xyl** (2.15 g, 10.1 mmol), and NaO^{t}Bu (1.46 g, 15.2 mmol) were added. The vial was capped and heated at 80 °C overnight while stirring. The vial was then removed from the glovebox, and the mixture was filtered through a plug of silica gel with 100 mL of a 1:4 mixture of methanol and ethyl acetate. The solvent was evaporated, and the residue was purified by flash chromatography on silica gel using a gradient of 0 to 20% methanol in dichloromethane. Yield: 2.53 g, 67%. ^{1}H NMR (C_6D_6): δ 7.69 (t, $^3J_{HH}$ = 7.9 Hz, 1H), 7.38 (d, $^3J_{HH}$ = 7.9 Hz, 1H), 7.33 (br s, 1H), 7.09 (t, $^3J_{HH}$ = 7.9 Hz, 1H), 7.02 (d, $^3J_{HH}$ = 7.6 Hz, 1H), 6.94 (t, $^3J_{HH}$ = 7.6 Hz, 1H), 6.90 (t, $^3J_{HH}$ = 7.6 Hz, 1H), 6.47 (s, 2H), 6.46 (s, 1H), 6.27 (d, $^3J_{HH}$ = 8.0 Hz, 1H), 5.88 (s, 1H), 3.64 (s, 2H), 2.46 (q, $^3J_{HH}$ = 7.2 Hz, 4H), 2.07 (s, 6H), 0.95 (t, $^3J_{HH}$ = 7.2 Hz, 6H). ^{13}C{^{1}H} NMR: δ 160.00, 156.97, 143.85, 138.58, 137.97, 137.70, 132.15, 124.87, 124.52, 122.78, 122.10, 119.57, 115.87, 113.10, 106.14, 59.71, 47.57, 21.20, 12.16. HRMS (EI+): calcd for $C_{24}H_{30}N_4$, 374.2470; found, 374.2467.

Synthesis of 4-dipp-^{i}Pr. To a 100 mL round-bottom flask were added **3-dipp-^{i}Pr** (1.42 g, 3.10 mmol), a stir bar, and triethyl orthoformate (14 mL). The reaction mixture was heated to 100 °C

DOI: 10.1021/acs.organomet.8b00470
Organometallics 2018, 37, 3286−3297

while stirring. A solution of concentrated hydrochloric acid (1.53 g, 15.5 mmol) in triethyl orthoformate (14 mL) was added dropwise to the heated flask over 10 min. ^{1}H NMR analysis indicated that the reaction was complete immediately after the addition, and the flask was allowed to cool to room temperature. Then 20 mL of $CHCl_3$ was added, and the solution was added dropwise to a rapidly stirring flask containing 200 mL of methyl *tert*-butyl ether. The product precipitated as a fine white powder. The hygroscopic solid was filtered and washed with methyl *tert*-butyl ether several times. The solid was dried under a stream of N_2 on the filter, transferred to a vial, and further dried under vacuum. Yield: 1.35 g, 75%. Note: two ^{1}H and ^{13}C signals were seen for the four methyl groups on the 2,6-diisopropylphenyl substituent because of hindered rotation about the N−C_{aryl} bond. Additionally, two ^{1}H and ^{13}C signals were seen for the four methyl groups on the RNH^{i}Pr$_2^+$ substituent, consistent with slow inversion at the nitrogen center. ^{1}H NMR ($CDCl_3$): δ 12.70 (br, 1H), 10.17 (br, 1H), 8.54 (br, 1H), 8.43 (br, 1H), 8.28 (br, 1H), 8.23 (br, 1H), 7.85 (br, 1H), 7.66 (t, $^3J_{HH}$ = 6.5 Hz, 1H), 7.58 (t, $^3J_{HH}$ = 7.8 Hz, 1H), 7.36 (d, $^3J_{HH}$ = 8.0 Hz, 2H), 7.24 (d, $^3J_{HH}$ = 8.1 Hz, 1H), 5.01 (br, 2H), 3.85 (br, 2H), 2.17 (br hept, $^3J_{HH}$ = 6.7 Hz, 2H), 1.48 (br, 12H), 1.19 (d, $^3J_{HH}$ = 6.5 Hz, 6H), 1.00 (d, $^3J_{HH}$ = 6.5 Hz, 6H). ^{13}C{^{1}H} NMR: δ 155.04, 145.94, 144.93, 144.63, 142.42, 133.68, 132.47, 129.48, 128.79, 128.76, 127.20, 127.04, 125.14, 117.17, 115.06, 113.61, 57.46, 52.22, 29.01, 24.71, 23.66, 19.15, 17.22. HRMS (ESI+): calcd for $C_{31}H_{41}N_4$ (M − 2H − 3Cl), 469.3331; found, 469.3326.

Synthesis of 4-dipp-Et. To a 250 mL round-bottom flask were added **3-dipp-Et** (3.82 g, 8.86 mmol), a stir bar, and triethyl orthoformate (40 mL). The reaction mixture was heated to 100 °C while stirring. A solution of concentrated hydrochloric acid (4.37 g, 44.3 mmol) in triethyl orthoformate (40 mL) was added dropwise to the heated flask over 20 min. ^{1}H NMR analysis indicated that the reaction was complete immediately after the addition, and the flask was allowed to cool to room temperature. Then 50 mL of $CHCl_3$ was added, and the solution was added dropwise to a rapidly stirring flask containing 500 mL of methyl *tert*-butyl ether. The product precipitated as a fine white powder. The hygroscopic solid was filtered and washed with methyl *tert*-butyl ether several times. The solid was dried under a stream of N_2 on the filter, transferred to a vial, and further dried under vacuum. Yield: 3.00 g, 63%. Note: two ^{1}H and ^{13}C signals were seen for the four methyl groups on the 2,6-diisopropylphenyl substituent because of hindered rotation about the N−C_{aryl} bond. ^{1}H NMR ($CDCl_3$): δ 12.53 (br, 1H), 11.41 (br, 1H), 8.65 (br, 1H), 8.50 (br, 1H), 8.28 (br, 2H), 7.89 (br, 1H), 7.68 (br t, 1H), 7.60 (t, $^3J_{HH}$ = 7.6 Hz, 1H), 7.38 (d, $^3J_{HH}$ = 7.6 Hz, 2H), 7.25 (d, $^3J_{HH}$ = 7.5 Hz, 1H), 4.93 (br, 2H), 3.97 (br, 2H), 2.20 (br, 2H), 1.42 (br, 6H), 1.22 (d, $^3J_{HH}$ = 6.5 Hz, 6H), 1.01 (d, $^3J_{HH}$ = 6.5 Hz, 6H). ^{13}C{^{1}H} NMR: δ 152.14, 145.82, 145.63, 143.90, 142.56, 133.63, 132.30, 129.52, 128.64 (two peaks overlapped), 127.04, 126.92, 124.97, 117.13, 115.94, 113.36, 55.58, 48.72, 28.87, 24.57, 23.60, 9.29. HRMS (ESI+): calcd for $C_{29}H_{37}N_4$ (M − 2H − 3Cl), 441.3018; found, 441.3009.

Synthesis of 4-dipp-Me. To a 250 mL round-bottom flask were added **3-dipp-Me** (0.803 g, 2.00 mmol), a stir bar, and triethyl orthoformate (20 mL). The reaction mixture was heated to 100 °C while stirring. A solution of concentrated hydrochloric acid (1.18 g, 12.0 mmol) in triethyl orthoformate (20 mL) was added dropwise to the heated flask over 20 min. After the addition, the flask was allowed to cool to room temperature. Then 20 mL of $CHCl_3$ was added, and the solution was added dropwise to a rapidly stirring flask containing 500 mL of methyl *tert*-butyl ether. The product precipitated as a fine white powder. The hygroscopic solid was filtered and washed with methyl *tert*-butyl ether several times. The solid was dried under a stream of N_2 on the filter, transferred to a vial, and further dried under vacuum. Yield: 0.738 g, 69%. Note: two ^{1}H and ^{13}C signals were seen for the four methyl groups on the 2,6-diisopropylphenyl substituent because of hindered rotation about the N−C_{aryl} bond. ^{1}H NMR ($CDCl_3$): δ 12.49 (s, 1H), 12.08 (s, 1H), 8.74 (d, $^3J_{HH}$ = 8.2 Hz, 1H), 8.54 (d, $^3J_{HH}$ = 7.2 Hz, 1H), 8.35 (t, $^3J_{HH}$ = 6.7 Hz, 1H), 8.25 (d, $^3J_{HH}$ = 7.0 Hz, 1H), 7.95 (t, $^3J_{HH}$ = 7.6 Hz, 1H), 7.73 (t, $^3J_{HH}$ = 7.8 Hz, 1H), 7.67 (t, $^3J_{HH}$ = 7.8 Hz, 1H), 7.45 (d, $^3J_{HH}$ = 7.9 Hz, 2H), 7.32 (d, $^3J_{HH}$ = 8.3 Hz, 1H), 5.12 (d, $^3J_{HH}$ = 5.0 Hz, 2H), 3.10 (d, $^3J_{HH}$ = 4.6 Hz, 6H), 2.25 (hept, $^3J_{HH}$ = 6.6 Hz, 2H), 1.30 (d, $^3J_{HH}$ = 6.7 Hz, 6H), 1.08 (d, $^3J_{HH}$ = 6.7 Hz, 6H). ^{13}C{^{1}H} NMR: δ 152.01, 146.07, 145.97, 144.10, 142.45, 133.96, 132.57, 129.69, 128.84, 128.69, 127.11, 127.06, 125.22, 116.91, 116.11, 113.68, 60.12, 43.47, 29.12, 24.79, 23.74. HRMS (ESI+): calcd for $C_{27}H_{33}N_4$ (M − 2H − 3Cl), 413.2705; found, 413.2693.

Synthesis of 4-Mes-^{i}Pr. To a 100 mL round-bottom flask were added **3-Mes-^{i}Pr** (1.48 g, 3.54 mmol), a stir bar, and triethyl orthoformate (15 mL). The reaction mixture was heated to 100 °C while stirring. A solution of concentrated hydrochloric acid (1.75 g, 17.7 mmol) in triethyl orthoformate (15 mL) was added dropwise to the heated flask over 10 min. ^{1}H NMR analysis indicated that the reaction was not complete, so another portion of hydrochloric acid (1.75 g) in triethyl orthoformate (15 mL) was added dropwise. The reaction was complete after the second addition, and the flask was allowed to cool to room temperature. Then 20 mL of $CHCl_3$ was added, and the solution was added dropwise to another rapidly stirring flask with 200 mL of methyl *tert*-butyl ether to yield an oil. The ether layer was decanted away, and the oil was dissolved in another 20 mL of $CHCl_3$, which was added dropwise to a rapidly stirring flask with 250 mL of methyl *tert*-butyl ether. The product precipitated as a fine pink powder. The hygroscopic solid was filtered and washed with methyl *tert*-butyl ether several times. The solid was dried under a stream of N_2 on the filter, transferred to a vial, and further dried under vacuum. Note: two ^{1}H and ^{13}C signals were seen for the four methyl groups on the RNH^{i}Pr$_2^+$ substituent, consistent with slow inversion at the nitrogen center. Yield: 1.36 g, 71%. ^{1}H NMR ($CDCl_3$): δ 12.64 (br, 1H), 10.12 (br, 1H), 8.53 (br, 1H), 8.38 (br, 1H), 8.28 (br, 1H), 8.21 (br, 1H), 7.83 (br, 1H), 7.67 (br t, 1H), 7.29 (d, $^3J_{HH}$ = 8.1 Hz, 1H), 7.06 (s, 2H), 5.02 (br, 2H), 3.89 (br, 2H), 2.33 (s, 3H), 2.03 (s, 6H), 1.51 (br d, 6H), 1.47 (br d, 6H). ^{13}C{^{1}H} NMR: δ 155.04, 145.15, 144.45, 142.43, 141.88, 134.72, 132.13, 130.36, 129.27, 129.07, 128.68, 127.66, 126.89, 116.99, 115.03, 113.84, 57.50, 52.17, 21.21, 19.16, 17.77, 17.33. HRMS (ESI+): calcd for $C_{28}H_{35}N_4$ (M − 2H − 3Cl), 427.2862; found, 427.2866.

Synthesis of 4-Xyl-Et. To a 100 mL round-bottom flask were added **4-Xyl-Et** (2.00 g, 5.34 mmol), a stir bar, and triethyl orthoformate (20 mL). The reaction mixture was heated to 100 °C while stirring. A solution of concentrated hydrochloric acid (2.63 g, 26.7 mmol) in triethyl orthoformate (20 mL) was added dropwise to the heated flask over 10 min. ^{1}H NMR analysis indicated that the reaction was complete immediately after the addition, and the flask was allowed to cool to room temperature. Then 20 mL of $CHCl_3$ was added, and the solution was added dropwise to another rapidly stirring flask with 100 mL of methyl *tert*-butyl ether to yield an oil. The liquid was decanted, and the oil was dissolved in another 20 mL of $CHCl_3$, which was added dropwise to a rapidly stirring flask with 200 mL of methyl *tert*-butyl ether. The product precipitated as a fine white powder. The hygroscopic solid was filtered and washed with methyl *tert*-butyl ether several times. The solid was dried under a stream of N_2 on the filter, transferred to a vial, and further dried under vacuum. Yield: 1.86 g, 70%. ^{1}H NMR ($CDCl_3$): δ 12.19 (br, 1H), 11.51 (br, 1H), 8.47 (d, $^3J_{HH}$ = 8.5 Hz, 1H), 8.39 (m, 3H), 8.26 (t, $^3J_{HH}$ = 7.7 Hz, 1H), 7.83 (m, 2H), 7.72 (t, $^3J_{HH}$ = 7.7 Hz, 1H), 7.49 (s, 2H), 7.21 (s, 1H), 4.93 (br, 2H), 3.35 (br q, 4H), 2.41 (s, 6H), 1.43 (t, $^3J_{HH}$ = 7.0 Hz, 6H). ^{13}C{^{1}H} NMR: δ 152.25, 146.01, 142.48, 142.22, 141.00, 132.96, 132.07, 131.89, 129.29 (two peaks overlapped), 128.51, 127.77, 122.45, 117.21, 115.49, 114.43, 55.57, 48.34, 21.34, 9.34. HRMS (ESI+): calcd for $C_{25}H_{29}N_4$ (M − 2H − 3Cl), 385.2392; found, 385.2398.

Synthesis of 5-Et. **1-Et** (1.73 g, 7.13 mmol), benzimidazole (0.843 g, 7.13 mmol), Cs_2CO_3 (4.65 g, 14.2 mmol), copper(I) iodide (0.135 g, 0.713 mmol), 8-hydroxyquinoline (0.144 g, 0.100 mmol), a stir bar, and acetonitrile (5 mL) were added to a 15 mL glass medium-pressure vessel in the glovebox. The vessel was capped, removed from the glovebox, and heated at 120 °C overnight while stirring. The vessel was opened, and the solvent was evaporated. The

DOI: 10.1021/acs.organomet.8b00470
Organometallics 2018, 37, 3286−3297

residue was purified by flash chromatography first on basic alumina using a gradient of 0 to 100% ethyl acetate in hexane, followed by a silica column using a gradient of 0 to 10% methanol in dichloromethane. Yield: 1.44 g, 72%. ^{1}H NMR ($CDCl_3$): δ 8.57 (s, 1H), 8.07 (d, $^3J_{HH}$ = 7.6 Hz, 1H), 7.85 (t, $^3J_{HH}$ = 7.6 Hz, 2H), 7.50 (d, $^3J_{HH}$ = 7.6 Hz, 1H), 7.41−7.32 (m, 3H), 3.81 (s, 2H), 2.63 (q, $^3J_{HH}$ = 7.0 Hz, 4H), 1.09 (t, $^3J_{HH}$ = 7.0 Hz, 6H). ^{13}C{^{1}H} NMR: δ 161.70, 149.09, 144.79, 141.53, 139.25, 132.32, 124.15, 123.25, 120.85, 120.70, 112.88, 112.12, 59.16, 47.65, 12.21. HRMS (ESI+): calcd for $C_{17}H_{21}N_4$ (M + H), 281.1766; found, 281.1767.

Synthesis of 4-^{i}Pr-Et. To a 150 mL glass medium-pressure vessel in the glovebox were added **5-Et** (2.15 g, 7.67 mmol), 2-bromopropane (18.9 g, 154 mmol), a stir bar, and acetonitrile (10 mL). The vessel was capped, removed from the glovebox, and heated at 120 °C overnight while stirring. The vessel was opened, and the solvent was evaporated. The residue was purified by flash chromatography on silica using a gradient of 0 to 40% methanol in dichloromethane. Yield: 2.14 g, 57%. ^{1}H NMR ($CDCl_3$): δ 11.61 (s, 1H), 10.43 (br, 1H), 8.30 (d, $^3J_{HH}$ = 8.0 Hz, 1H), 8.19 (br, 3H), 7.93 (d, $^3J_{HH}$ = 8.0 Hz, 1H), 7.74−7.65 (m, 2H), 5.21 (hept, $^3J_{HH}$ = 6.6 Hz, 1H), 4.84 (br, 2H), 3.32 (br, 4H), 1.85 (d, $^3J_{HH}$ = 6.6 Hz, 6H), 1.39 (br t, 6H). ^{13}C{^{1}H} NMR: δ 151.93 (br), 145.96, 142.19, 140.92, 131.00, 129.26, 128.83, 127.93, 126.73, 116.90, 115.13, 114.10, 55.53, 52.97, 48.55, 22.28, 9.41. HRMS (ESI+): calcd for $C_{20}H_{27}N_4$ (M − H − 2Br), 323.2236; found, 323.2233.

Synthesis of Ru-dipp-^{i}Pr. In the glovebox, the trihydrochloride salt **4-dipp-^{i}Pr** (300 mg, 0.519 mmol), a stir bar, 3.5 Å molecular sieves (1.2 g), Ag_2O (601 mg, 2.59 mmol), and THF (10 mL) were added to a vial, and the mixture was stirred at room temperature for 1.5 h in the dark. The mixture was filtered through a PTFE filter disk into a vial containing $RuHCl(CO)(PPh_3)_3$ (494 mg, 0.519 mmol) and AgCl (2.23 g, 15.6 mmol). The reaction mixture was stirred and heated at 50 °C overnight. The crude reaction mixture was then purified by air-free flash chromatography using a gradient of 0 to 100% ethyl acetate in dichloromethane. Material purified in this manner was pure by NMR spectroscopy, but catalytic trials were conducted using samples that were further purified by recrystallization: a solution in dichloromethane was first layered with a small amount of toluene and then an excess of pentane. Yield after recrystallization: 156 mg, 47%. ^{1}H NMR (CD_2Cl_2, assignments correspond to Figure S35): δ 7.88−7.80 (m, 1H, H_n), 7.77 (d, $^3J_{HH}$ = 8.2 Hz, 1H, H_m), 7.74 (d, $^3J_{HH}$ = 8.2 Hz, 1H, H_l), 7.49 (t, $^3J_{HH}$ = 7.8 Hz, 1H, H_e), 7.36 (dd, $^3J_{HH}$ = 7.8 Hz, $^4J_{HH}$ = 1.4 Hz, 1H, H_f), 7.27 (dd, $^3J_{HH}$ = 7.8 Hz, $^4J_{HH}$ = 1.4 Hz, 1H, H_d), 7.23−7.15 (m, 1H, H_k), 7.14−7.06 (m, 1H, H_j), 7.02 (d, $^3J_{HH}$ = 7.5 Hz, 1H, H_o), 6.64−6.58 (d, $^3J_{HH}$ = 7.7 Hz, 1H, H_i), 4.65 (d, $^2J_{HH}$ = 15.6 Hz, 1H, H_{pCl}), 4.19−4.11 (m, 1H, H_s), 4.03 (d, $^2J_{HH}$ = 15.6 Hz, 1H, H_{pH}), 3.09 (hept, $^3J_{HH}$ = 6.4 Hz, 1H, H_q), 2.91 (hept, $^3J_{HH}$ = 6.8 Hz, 1H, H_g), 2.29 (hept, $^3J_{HH}$ = 6.8 Hz, 1H, H_b), 1.41 (d, $^3J_{HH}$ = 6.9 Hz, 3H, H_t), 1.32 (d, $^3J_{HH}$ = 6.7 Hz, 3H, H_h), 1.18 (d, $^3J_{HH}$ = 6.8 Hz, 3H, H_t), 1.16 (d, $^3J_{HH}$ = 6.8 Hz, 3H, H_c), 1.09 (d, $^3J_{HH}$ = 6.3 Hz, 3H, H_r), 1.01 (d, $^3J_{HH}$ = 6.5 Hz, 3H, H_r), 0.89 (d, $^3J_{HH}$ = 6.9 Hz, 3H, H_h), 0.84 (d, $^3J_{HH}$ = 6.9 Hz, 3H, H_c), −14.31 (s, 1H, H_a). Residual CH_2Cl_2 was observed, integrating to 0.5 molar equiv. ^{13}C{^{1}H} NMR: δ 215.12, 206.27, 163.22, 150.43, 148.75, 147.90, 139.21, 138.61, 132.86, 131.48, 130.74, 124.95, 123.70, 122.87, 115.60, 110.48, 110.22, 108.59, 63.29, 59.62, 57.38, 28.82, 28.66, 26.00, 25.15, 24.89, 23.95, 23.66, 23.44, 22.99, 18.44. The two meta hydrogens on the dipp group (d and e in the Supporting Information) have overlapping ^{13}C signals at 124.95 ppm, which was verified by HMQC experiments. Recrystallized samples retained dichloromethane upon drying, as verified by ^{1}H NMR analysis. Anal. Calcd for $C_{32}H_{41}N_4ClORu{\cdot}0.5(CH_2Cl_2)$: C, 57.68; H, 6.26; N, 8.28. Found: C, 57.78; H, 6.45; N, 8.32.

Synthesis of Ru-dipp-Et. In the glovebox, the trihydrochloride salt **4-dipp-Et** (600 mg, 1.09 mmol), a stir bar, 3.5 Å molecular sieves (2.0 g), Ag_2O (1.26 g, 5.45 mmol), and CH_2Cl_2 (20 mL) were added to a vial, and the mixture was stirred at room temperature for 2 h in the dark. The mixture was filtered through a PTFE filter disk into a vial containing $RuHCl(CO)(PPh_3)_3$ (1.04 g, 1.09 mmol) and AgCl (1.56 g, 10.9 mmol). The reaction mixture was stirred and heated at 40 °C for 2 days. The crude reaction mixture was then purified by air-free flash chromatography using a gradient of 0 to 100% ethyl acetate in dichloromethane. Material purified in this manner was pure by NMR spectroscopy, but catalytic trials were conducted using samples that were further purified by recrystallization: a solution in dichloromethane was first layered with a small amount of toluene and then an excess of pentane. Yield after recrystallization: 374 mg, 56%. ^{1}H NMR (CD_2Cl_2, assignments correspond to Figure S37): δ 8.03−7.90 (m, 2H, $H_{n,m}$), 7.86 (d, $^3J_{HH}$ = 8.1 Hz, 1H, H_l), 7.61 (t, $^3J_{HH}$ = 7.8 Hz, 1H, H_e), 7.49 (dd, $^3J_{HH}$ = 7.8 Hz, $^4J_{HH}$ = 1.3 Hz, 1H, H_f), 7.39 (dd, $^3J_{HH}$ = 7.7 Hz, $^4J_{HH}$ = 1.3 Hz, 1H, H_d), 7.31 (t, $^3J_{HH}$ = 8.1 Hz, 1H, H_k), 7.28−7.16 (m, 2H, $H_{j,o}$), 6.74 (d, $^3J_{HH}$ = 7.9 Hz, 1H, H_i), 4.84 (d, $^2J_{HH}$ = 14.9 Hz, 1H, H_{pCl}), 3.95 (d, $^2J_{HH}$ = 14.9 Hz, 1H, H_{pH}), 3.60 (dq, $^2J_{HH}$ = 14.1 Hz, $^3J_{HH}$ = 7.1 Hz, 1H, H_s), 3.34 (dq, $^2J_{HH}$ = 14.3 Hz, $^3J_{HH}$ = 7.2 Hz, 1H, H_s), 3.04 (hept, $^3J_{HH}$ = 6.8 Hz, 1H, H_g), 2.85 (m, 2H, H_q), 2.42−2.31 (m, 1H, H_b), 1.42 (d, $^3J_{HH}$ = 6.7 Hz, 3H, H_h), 1.25 (d, $^3J_{HH}$ = 6.8 Hz, 3H, H_c), 1.18 (t, $^3J_{HH}$ = 7.0 Hz, 3H, H_r), 1.11 (t, $^3J_{HH}$ = 7.2 Hz, 3H, H_t), 1.01 (d, $^3J_{HH}$ = 6.9 Hz, 3H, H_h), 0.95 (d, $^3J_{HH}$ = 6.9 Hz, 3H, H_c), −14.58 (s, 1H, H_a). ^{13}C{^{1}H} NMR: δ 215.70, 205.65, 160.10, 150.92, 148.64, 147.79, 138.95, 138.56, 132.91, 131.52, 130.67, 124.91, 123.72, 122.90, 116.92, 110.55, 110.25, 109.28, 64.35, 54.61, 49.97, 28.81, 28.63, 25.14, 24.81, 23.85, 23.69, 11.34, 8.93. The two meta carbons on the dipp ring (d and e in the Supporting Information) have overlapping ^{13}C signals at 124.91 ppm, which was verified by COSY experiments. Anal. Calcd for $C_{30}H_{37}N_4ClORu$: C, 59.44; H, 6.15; N, 9.24. Found: C, 59.62; H, 6.17; N, 9.17.

Synthesis of Ru-dipp-Me. The synthesis, chromatographic purification, and recrystallization of **Ru-dipp-Me** were performed in an analogous fashion to **Ru-dipp-Et**, starting with **4-dipp-Me** (200 mg, 0.383 mmol). Yield after recrystallization: 110 mg, 50%. ^{1}H NMR (CD_2Cl_2, assignments correspond to Figure S39): δ 7.93−7.80 (m, 2H, $H_{n,m}$), 7.75 (d, $^3J_{HH}$ = 8.1 Hz, 1H, H_l), 7.49 (t, $^3J_{HH}$ = 7.8 Hz, 1H, H_e), 7.36 (dd, $^3J_{HH}$ = 7.8 Hz, $^4J_{HH}$ = 1.4 Hz, 1H, H_f), 7.27 (dd, $^3J_{HH}$ = 7.8 Hz, $^4J_{HH}$ = 1.4 Hz, 1H, H_d), 7.20 (td, $^3J_{HH}$ = 7.9 Hz, $^4J_{HH}$ = 1.1 Hz, 1H, H_k), 7.10 (m, 2H, $H_{j,o}$), 6.62 (d, $^3J_{HH}$ = 7.7 Hz, 1H, H_i), 4.81 (d, $^2J_{HH}$ = 14.8 Hz, 1H, H_{pCl}), 3.46 (d, $^2J_{HH}$ = 14.8 Hz, 1H, H_{pH}), 2.97−2.84 (m, 4H, $H_{g,r}$), 2.66 (s, 3H, H_q), 2.23 (hept, $^3J_{HH}$ = 6.8 Hz, 1H, H_b), 1.29 (d, $^3J_{HH}$ = 6.7 Hz, 3H, H_h), 1.11 (d, $^3J_{HH}$ = 6.8 Hz, 3H, H_c), 0.86 (d, $^3J_{HH}$ = 6.9 Hz, 3H, H_c), 0.84 (d, $^3J_{HH}$ = 6.9 Hz, 3H, H_c), −14.58 (s, 1H, H_a). Residual CH_2Cl_2 was observed, integrating to 0.5 molar equiv. ^{13}C{^{1}H} NMR: δ 215.39, 204.88, 159.18, 150.67, 148.21, 147.32, 138.56, 138.13, 132.48, 131.17, 130.27, 124.50, 124.48, 123.37, 122.53, 116.47, 110.20, 109.86, 109.15, 68.86, 58.27, 51.43, 28.41, 28.21, 24.78, 24.38, 23.41, 23.35. Recrystallized samples retained dichloromethane upon drying, as verified by ^{1}H NMR analysis. Anal. Calcd for $C_{28}H_{33}ClN_4ORu{\cdot}0.5(CH_2Cl_2)$: C, 55.15; H, 5.52; N, 9.03. Found: C, 55.05; H, 5.72; N, 8.87.

Synthesis of Ru-Mes-^{i}Pr. The synthesis, chromatographic purification, and recrystallization of **Ru-Mes-^{i}Pr** were performed in an analogous fashion to **Ru-dipp-Et**, starting with **4-Mes-^{i}Pr** (300 mg, 0.560 mmol), except that the transmetalation step was carried out at room temperature instead of 40 °C. Yield after recrystallization: 171 mg, 52%. ^{1}H NMR (CD_2Cl_2, assignments correspond to Figure S41): δ 8.00 (t, $^3J_{HH}$ = 7.8 Hz, 1H, H_l), 7.91−7.80 (m, 2H, $H_{k,j}$), 7.38−7.28 (t, $^3J_{HH}$ = 7.7 Hz, 1H, H_i), 7.27−7.20 (m, 2H, $H_{h,m}$), 7.18 (s, 1H, H_e), 7.11 (s, 1H, H_c), 6.80−6.69 (d, $^3J_{HH}$ = 7.2 Hz, 1H, H_g), 4.72 (d, $^2J_{HH}$ = 15.6 Hz, 1H, H_{nCl}), 4.31 (hept, $^3J_{HH}$ = 6.5 Hz, 1H, H_q), 4.17 (d, $^2J_{HH}$ = 15.6 Hz, 1H, H_{nH}), 3.24 (hept, $^3J_{HH}$ = 6.5 Hz, 1H, H_o), 2.44 (s, 3H, H_d), 2.24 (s, 3H, H_f), 2.00 (s, 3H, H_b), 1.54 (d, $^3J_{HH}$ = 6.9 Hz, 3H, H_r), 1.30 (d, $^3J_{HH}$ = 6.9 Hz, 3H, H_r), 1.22 (d, $^3J_{HH}$ = 6.3 Hz, 3H, H_p), 1.14 (d, $^3J_{HH}$ = 6.5 Hz, 3H, H_p), −14.31 (s, 1H, H_a). Residual CH_2Cl_2 was observed, integrating to 1.0 molar equiv. ^{13}C{^{1}H} NMR: δ 215.70, 205.65, 160.10, 150.92, 148.64, 147.79, 138.95, 138.56, 132.91, 131.52, 130.67, 124.91, 123.72, 122.90, 116.92, 110.55, 110.25, 109.28, 64.35, 54.61, 49.97, 28.81, 28.63, 25.14, 24.81, 23.85, 23.69, 11.34, 8.93. Recrystallized samples retained dichloromethane upon drying, as verified by ^{1}H NMR analysis. The peak for CH_2Cl_2

DOI: 10.1021/acs.organomet.8b00470
Organometallics 2018, 37, 3286−3297

Anal. Calcd for $C_{29}H_{35}N_4ClORu \bullet CH_2Cl_2$: C, 53.21; H, 5.51; N, 8.27. Found: C, 53.40; H, 5.60; N, 8.30.

Synthesis of Ru-Xyl-Et. The synthesis, chromatographic purification, and recrystallization of **Ru-Xyl-Et** were performed in an analogous fashion to **Ru-dipp-Et**, starting with **4-Xyl-Et** (180 mg, 0.36 mmol), except that the transmetalation step was complete after 2 h at room temperature. Yield after recrystallization: 76 mg, 38%. ^{1}H NMR (CD_2Cl_2, assignments correspond to Figure S43): δ 7.92 (m, 2H, $H_{i,k}$), 7.84 (d, $^3J_{HH}$ = 8.0 Hz, 1H, H_j), 7.68 (s, 1H, H_f), 7.30 (td, $^3J_{HH}$ = 7.7 Hz, $^4J_{HH}$ = 1.3 Hz, 1H, H_i), 7.26 (s, 1H, H_d), 7.23 (td, $^3J_{HH}$ = 7.7 Hz, $^4J_{HH}$ = 1.0 Hz, 1H, H_h), 7.21−7.17 (m, 1H, H_m), 7.15 (s, 1H, H_b), 7.09 (dd, $^3J_{HH}$ = 8.1 Hz, $^4J_{HH}$ = 1.2 Hz, 1H, H_g), 4.79 (d, $^2J_{HH}$ = 15.0 Hz, 1H, H_{nCl}), 3.98 (d, $^2J_{HH}$ = 14.8 Hz, 1H, H_{nH}), 3.61 (dq, $^2J_{HH}$ = 14.2 Hz, $^3J_{HH}$ = 7.1 Hz, 1H, H_p), 3.40 (dq, $^2J_{HH}$ = 14.4 Hz, $^3J_{HH}$ = 7.2 Hz, 1H, H_p), 3.00−2.75 (m, 2H, H_o), 2.53 (s, 3H, H_e), 2.48 (s, 3H, H_c), 1.16 (q, $^3J_{HH}$ = 7.2 Hz, 3H, H_r), 1.14 (q, $^3J_{HH}$ = 7.2 Hz, 3H, H_q), −14.74 (s, 1H, H_a). $^{13}C\{^1H\}$ NMR: δ 214.16, 206.28, 159.82, 151.02, 140.64, 139.42, 138.99, 137.94, 137.62, 131.67, 130.95, 128.22, 124.73, 123.72, 123.17, 117.04, 110.42, 110.19, 109.40, 64.51, 54.86, 50.36, 21.59, 21.40, 11.31, 9.11. The samples synthesized contained $Ag_4Cl_4(PPh_3)_4$ and other unidentified impurities, which could not be completely removed by chromatography or recrystallization. Signals for $Ag_4Cl_4(PPh_3)_4$ were observed at 7.51−7.37 ppm in the ^{1}H NMR spectrum and at 134.31 (d, J = 16.6 Hz) and 129.37 (d, J = 10.0 Hz) in the ^{13}C NMR spectrum. Satisfactory elemental analysis could not be obtained. HRMS (ESI+): calcd for $C_{26}H_{29}N_4ORu$ (M − Cl), 515.1385; found, 515.1385.

Synthesis of Ru-^{i}Pr-Et. The synthesis, chromatographic purification, and recrystallization of **Ru-^{i}Pr-Et** were performed in an analogous fashion to **Ru-dipp-Et**, starting with **4-^{i}Pr-Et**, except that the transmetalation step was complete after 1 day at room temperature. Yield after recrystallization: 35 mg, 16%. ^{1}H NMR (CD_2Cl_2, assignments correspond to Figure S45): δ 7.94 (t, $^3J_{HH}$ = 8.2 Hz, 1H, H_i), 7.81 (d, $^3J_{HH}$ = 8.4 Hz, 1H, H_h), 7.78 (dd, $^3J_{HH}$ = 6.0, 3.2 Hz, 1H, H_g), 7.55 (dd, $^3J_{HH}$ = 6.0, 3.2 Hz, 1H, H_d), 7.26 (dd, $^3J_{HH}$ = 6.1, 3.2 Hz, 2H, $H_{e,f}$), 7.19 (d, $^3J_{HH}$ = 7.6 Hz, 1H, H_j), 5.64 (hept, $^3J_{HH}$ = 7.2 Hz, 1H, H_b), 4.78 (d, $^2J_{HH}$ = 14.8 Hz, 1H, H_{kCl}), 3.94 (d, $^3J_{HH}$ = 14.8 Hz, 1H, H_{kH}), 3.68 (m, 1H, H_n), 3.45 (m, 1H, H_n), 3.06−2.72 (m, 2H, H_l), 1.76 (d, $^3J_{HH}$ = 7.1 Hz, 3H, H_c), 1.70 (d, $^3J_{HH}$ = 7.1 Hz, 3H, H_c), 1.21 (t, $^3J_{HH}$ = 7.0 Hz, 3H, H_m), 1.16 (t, $^3J_{HH}$ = 7.2 Hz, 3H, H_o), −14.95 (s, 1H, H_a). $^{13}C\{^1H\}$ NMR: δ 212.96, 208.90, 159.98, 151.36, 139.33, 134.39, 133.11, 123.39, 122.91, 117.23, 111.82, 110.72, 109.43, 64.87, 55.41, 54.45, 50.71, 21.23, 20.54, 11.71, 9.13. The sample synthesized contained a very small but detectable amount of an impurity tentatively assigned as $Ag_4Cl_4(PPh_3)_4$, which could not be completely removed by chromatography or recrystallization. This impurity appeared as a multiplet at 7.51−7.37 ppm in the ^{1}H NMR spectrum. Satisfactory elemental analysis could not be obtained. HRMS (ESI+): calcd for $C_{21}H_{27}N_4ORu$ (M − Cl), 453.1228; found, 453.1231.

General Procedure for Hydrogenation. In an argon-filled glovebox, the ruthenium complex and NaO^{t}Bu were dissolved in toluene and heated with stirring at 50 °C for about an hour, after which a homogeneous orange solution formed. Next, the ester, dissolved in toluene, was combined with the catalyst in a test tube containing a stir bar. The tube was placed in a stainless steel pressure reactor inside the glovebox, which was subsequently sealed and brought out. Then the reactor was pressurized with 6 bar H_2 and vented three times to remove the argon atmosphere, and finally it was filled with 6 bar H_2. The reactor was heated at 105 °C with stirring for 20 h, after which it was allowed to cool for 1 h before being vented carefully and opened. An aliquot of the reaction mixture was taken and analyzed by ^{1}H NMR spectroscopy in $CDCl_3$ and/or gas chromatography.

■ ASSOCIATED CONTENT

Supporting Information

The Supporting Information is available free of charge on the ACS Publications website at DOI: 10.1021/acs.organomet.8b00470.

Experimental procedures for X-ray crystallography and isolation of catalytic products, images of NMR spectra for all new compounds, and detailed NMR assignments for all ruthenium complexes (PDF)

Accession Codes

CCDC 1852064−1852069 contain the supplementary crystallographic data for this paper. These data can be obtained free of charge via www.ccdc.cam.ac.uk/data_request/cif, or by e-mailing data_request@ccdc.cam.ac.uk, or by contacting The Cambridge Crystallographic Data Centre, 12 Union Road, Cambridge CB2 1EZ, U.K.; fax: +44 1223 336033.

■ AUTHOR INFORMATION

Corresponding Author

*E-mail: achianese@colgate.edu.

ORCID

Daniel Kim: 0000-0001-6464-3804

Anthony R. Chianese: 0000-0002-9140-6115

Notes

The authors declare no competing financial interest.

■ ACKNOWLEDGMENTS

We thank the National Science Foundation for support of the research project (CHE-1362501) and for the acquisition of an upgraded NMR spectrometer (CHE-1726308).

■ REFERENCES

(1) (a) Turek, T.; Trimm, D. L.; Cant, N. W. The Catalytic Hydrogenolysis of Esters to Alcohols. *Catal. Rev.: Sci. Eng.* **1994**, *36*, 645−683. (b) Rieke, R.; Thakur, D.; Roberts, B.; White, G. Fatty Methyl Ester Hydrogenation to Fatty Alcohol Part II: Process Issues. *J. Am. Oil Chem. Soc.* **1997**, *74*, 341−345. (c) Rieke, R.; Thakur, D.; Roberts, B.; White, G. Fatty Methyl Ester Hydrogenation to Fatty Alcohol Part I: Correlation between Catalyst Properties and Activity/Selectivity. *J. Am. Oil Chem. Soc.* **1997**, *74*, 333−339. (d) Pouilloux, Y.; Autin, F.; Barrault, J. Selective Hydrogenation of Methyl Oleate into Unsaturated Alcohols: Relationships between Catalytic Properties and Composition of Cobalt−Tin Catalysts. *Catal. Today* **2000**, *63*, 87−100.

(2) (a) Grey, R. A.; Pez, G. P.; Wallo, A. Anionic Metal Hydride Catalysts. 2. Application to the Hydrogenation of Ketones, Aldehydes, Carboxylic Acid Esters, and Nitriles. *J. Am. Chem. Soc.* **1981**, *103*, 7536−7542. (b) Matteoli, U.; Menchi, G.; Bianchi, M.; Piacenti, F. Homogeneous Catalytic Hydrogenation Dicarboxylic Acid Esters. II. *J. Organomet. Chem.* **1986**, *299*, 233−238. (c) Hara, Y.; Inagaki, H.; Nishimura, S.; Wada, K. Selective Hydrogenation of Cyclic Ester to α,Ω-Diol Catalyzed by Cationic Ruthenium Complexes with Trialkylphosphine Ligands. *Chem. Lett.* **1992**, *21*, 1983−1986. (d) Teunissen, H. T.; Elsevier, C. J. Homogeneous Ruthenium Catalyzed Hydrogenation of Esters to Alcohols. *Chem. Commun.* **1998**, 1367−1368. (e) Nomura, K.; Ogura, H.; Imanishi, Y. Direct Synthesis of 2-Phenylethanol by Hydrogenation of Methyl Phenylacetate Using Homogeneous Ruthenium-Phosphine Catalysis under Low Hydrogen Pressure. *J. Mol. Catal. A: Chem.* **2001**, *166*, 345−349.

(3) Zhang, J.; Leitus, G.; Ben-David, Y.; Milstein, D. Efficient Homogeneous Catalytic Hydrogenation of Esters to Alcohols. *Angew. Chem., Int. Ed.* **2006**, *45*, 1113−1115.

(4) (a) Saudan, L. A.; Saudan, C. M.; Debieux, C.; Wyss, P. Dihydrogen Reduction of Carboxylic Esters to Alcohols under the

DOI: 10.1021/acs.organomet.8b00470
Organometallics 2018, 37, 3286−3297

Catalysis of Homogeneous Ruthenium Complexes: High Efficiency and Unprecedented Chemoselectivity. *Angew. Chem., Int. Ed.* **2007**, *46*, 7473−7476. (b) Fogler, E.; Balaraman, E.; Ben-David, Y.; Leitus, G.; Shimon, L. J. W.; Milstein, D. New CNN-Type Ruthenium Pincer NHC Complexes. Mild, Efficient Catalytic Hydrogenation of Esters. *Organometallics* **2011**, *30*, 3826−3833. (c) Kuriyama, W.; Matsumoto, T.; Ogata, O.; Ino, Y.; Aoki, K.; Tanaka, S.; Ishida, K.; Kobayashi, T.; Sayo, N.; Saito, T. Catalytic Hydrogenation of Esters. Development of an Efficient Catalyst and Processes for Synthesising (R)-1,2-Propanediol and 2-(L-Menthoxy)Ethanol. *Org. Process Res. Dev.* **2012**, *16*, 166−171. (d) Spasyuk, D.; Gusev, D. G. Acceptorless Dehydrogenative Coupling of Ethanol and Hydrogenation of Esters and Imines. *Organometallics* **2012**, *31*, 5239−5242. (e) Spasyuk, D.; Smith, S.; Gusev, D. G. From Esters to Alcohols and Back with Ruthenium and Osmium Catalysts. *Angew. Chem., Int. Ed.* **2012**, *51*, 2772−2775. (f) O, W. W. N.; Morris, R. H. Ester Hydrogenation Catalyzed by a Ruthenium(II) Complex Bearing an N-Heterocyclic Carbene Tethered with an "NH_2" Group and a DFT Study of the Proposed Bifunctional Mechanism. *ACS Catal.* **2013**, *3*, 32−40. (g) Spasyuk, D.; Smith, S.; Gusev, D. G. Replacing Phosphorus with Sulfur for the Efficient Hydrogenation of Esters. *Angew. Chem., Int. Ed.* **2013**, *52*, 2538−2542. (h) Yang, X. H.; Xie, J. H.; Liu, W. P.; Zhou, Q. L. Catalytic Asymmetric Hydrogenation of Delta-Ketoesters: Highly Efficient Approach to Chiral 1,5-Diols. *Angew. Chem., Int. Ed.* **2013**, *52*, 7833−7836. (i) Filonenko, G. A.; Cosimi, E.; Lefort, L.; Conley, M. P.; Copéret, C.; Lutz, M.; Hensen, E. J. M.; Pidko, E. A. Lutidine-Derived Ru-CNC Hydrogenation Pincer Catalysts with Versatile Coordination Properties. *ACS Catal.* **2014**, *4*, 2667−2671. (j) Yang, X. H.; Wang, K.; Zhu, S. F.; Xie, J. H.; Zhou, Q. L. Remote Ester Group Leads to Efficient Kinetic Resolution of Racemic Aliphatic Alcohols Via Asymmetric Hydrogenation. *J. Am. Chem. Soc.* **2014**, *136*, 17426−17429. (k) Fairweather, N. T.; Gibson, M. S.; Guan, H. Homogeneous Hydrogenation of Fatty Acid Methyl Esters and Natural Oils under Neat Conditions. *Organometallics* **2015**, *34*, 335−339. (l) Filonenko, G. A.; Aguila, M. J. B.; Schulpen, E. N.; van Putten, R.; Wiecko, J.; Müller, C.; Lefort, L.; Hensen, E. J. M.; Pidko, E. A. Bis-N-Heterocyclic Carbene Aminopincer Ligands Enable High Activity in Ru-Catalyzed Ester Hydrogenation. *J. Am. Chem. Soc.* **2015**, *137*, 7620−7623. (m) Korstanje, T. J.; van der Vlugt, J. I.; Elsevier, C. J.; de Bruin, B. Hydrogenation of Carboxylic Acids with a Homogeneous Cobalt Catalyst. *Science* **2015**, *350*, 298−302. (n) Spasyuk, D.; Vicent, C.; Gusev, D. G. Chemoselective Hydrogenation of Carbonyl Compounds and Acceptorless Dehydrogenative Coupling of Alcohols. *J. Am. Chem. Soc.* **2015**, *137*, 3743−3746. (o) Tan, X.; Wang, Q.; Liu, Y.; Wang, F.; Lv, H.; Zhang, X. A New Designed Hydrazine Group-Containing Ruthenium Complex Used for Catalytic Hydrogenation of Esters. *Chem. Commun.* **2015**, *51*, 12193−12196. (p) Tan, X.; Wang, Y.; Liu, Y.; Wang, F.; Shi, L.; Lee, K. H.; Lin, Z.; Lv, H.; Zhang, X. Highly Efficient Tetradentate Ruthenium Catalyst for Ester Reduction: Especially for Hydrogenation of Fatty Acid Esters. *Org. Lett.* **2015**, *17*, 454−457. (q) Ogata, O.; Nakayama, Y.; Nara, H.; Fujiwhara, M.; Kayaki, Y. Atmospheric Hydrogenation of Esters Catalyzed by PNP-Ruthenium Complexes with an N-Heterocyclic Carbene Ligand. *Org. Lett.* **2016**, *18*, 3894−3897. (r) Stadler, B. M.; Puylaert, P.; Diekamp, J.; van Heck, R.; Fan, Y.; Spannenberg, A.; Hinze, S.; de Vries, J. G. Inexpensive Ruthenium NNS-Complexes as Efficient Ester Hydrogenation Catalysts with High C═O vs. C═C Selectivities. *Adv. Synth. Catal.* **2018**, *360*, 1151−1158. (s) Widegren, M. B.; Clarke, M. L. Manganese Catalyzed Hydrogenation of Enantiomerically Pure Esters. *Org. Lett.* **2018**, *20*, 2654−2658.

(5) (a) Herrmann, W. A.; Köcher, C. N-Heterocyclic Carbenes. *Angew. Chem., Int. Ed. Engl.* **1997**, *36*, 2162−2187. (b) Bourissou, D.; Guerret, O.; Gabbaï, F. P.; Bertrand, G. Stable Carbenes. *Chem. Rev.* **2000**, *100*, 39−91.

(6) Diez-Gonzalez, S.; Marion, N.; Nolan, S. P. N-Heterocyclic Carbenes in Late Transition Metal Catalysis. *Chem. Rev.* **2009**, *109*, 3612−3676.

(7) (a) del Pozo, C.; Iglesias, M.; Sánchez, F. l. Pincer-Type Pyridine-Based N-Heterocyclic Carbene Amine Ru(II) Complexes as Efficient Catalysts for Hydrogen Transfer Reactions. *Organometallics* **2011**, *30*, 2180−2188. (b) Sun, Y.; Koehler, C.; Tan, R.; Annibale, V. T.; Song, D. Ester Hydrogenation Catalyzed by Ru-CNN Pincer Complexes. *Chem. Commun.* **2011**, *47*, 8349−8351. (c) Westerhaus, F. A.; Wendt, B.; Dumrath, A.; Wienhofer, G.; Junge, K.; Beller, M. Ruthenium Catalysts for Hydrogenation of Aromatic and Aliphatic Esters: Make Use of Bidentate Carbene Ligands. *ChemSusChem* **2013**, *6*, 1001−1005. (d) Sluijter, S. N.; Korstanje, T. J.; van der Vlugt, J. I.; Elsevier, C. J. Mechanistic Insights into Catalytic Carboxylic Ester Hydrogenation with Cooperative Ru(II)-Bis{1,2,3-Triazolylidene}-Pyridine Pincer Complexes. *J. Organomet. Chem.* **2017**, *845*, 30−37.

(8) Kim, D.; Le, L.; Drance, M. J.; Jensen, K. H.; Bogdanovski, K.; Cervarich, T. N.; Barnard, M. G.; Pudalov, N. J.; Knapp, S. M. M.; Chianese, A. R. Ester Hydrogenation Catalyzed by CNN-Pincer Complexes of Ruthenium. *Organometallics* **2016**, *35*, 982−989.

(9) Cross, W. B.; Daly, C. G.; Ackerman, R. L.; George, I. R.; Singh, K. N-Heterocyclic Carbene Tethered Amido Complexes of Palladium and Platinum. *Dalton Trans.* **2011**, *40*, 495−505.

(10) Wang, H. M. J.; Lin, I. J. B. Facile Synthesis of Silver(I)-Carbene Complexes. Useful Carbene Transfer Agents. *Organometallics* **1998**, *17*, 972−975.

(11) Teo, B.-K.; Calabrese, J. C. Stereochemical Systematics of Metal Clusters. Structural Characterization of Tetrameric Triphenylphosphine Silver Chloride. An Analysis of Bonded vs. Nonbonded Interactions in the Cubane-Like $(R_3Y)_4M_4X_4$ Species. *Inorg. Chem.* **1976**, *15*, 2467−2474.

(12) (a) Zhang, J.; Leitus, G.; Ben-David, Y.; Milstein, D. Facile Conversion of Alcohols into Esters and Dihydrogen Catalyzed by New Ruthenium Complexes. *J. Am. Chem. Soc.* **2005**, *127*, 10840−10841. (b) Gunanathan, C.; Shimon, L. J.; Milstein, D. Direct Conversion of Alcohols to Acetals and H_2 Catalyzed by an Acridine-Based Ruthenium Pincer Complex. *J. Am. Chem. Soc.* **2009**, *131*, 3146−3147. (c) Salem, H.; Shimon, L. J. W.; Diskin-Posner, Y.; Leitus, G.; Ben-David, Y.; Milstein, D. Formation of Stabletrans-Dihydride Ruthenium(II) and 16-Electron Ruthenium(0) Complexes Based on Phosphinite PONOP Pincer Ligands. Reactivity toward Water and Electrophiles. *Organometallics* **2009**, *28*, 4791−4806. (d) Balaraman, E.; Gnanaprakasam, B.; Shimon, L. J. W.; Milstein, D. Direct Hydrogenation of Amides to Alcohols and Amines under Mild Conditions. *J. Am. Chem. Soc.* **2010**, *132*, 16756−16758. (e) Chen, T.; He, L.-P.; Gong, D.; Yang, L.; Miao, X.; Eppinger, J.; Huang, K.-W. Ruthenium(II) Pincer Complexes with Oxazoline Arms for Efficient Transfer Hydrogenation Reactions. *Tetrahedron Lett.* **2012**, *53*, 4409−4412. (f) Gargir, M.; Ben-David, Y.; Leitus, G.; Diskin-Posner, Y.; Shimon, L. J. W.; Milstein, D. PNS-Type Ruthenium Pincer Complexes. *Organometallics* **2012**, *31*, 6207−6214. (g) Barrios-Francisco, R.; Balaraman, E.; Diskin-Posner, Y.; Leitus, G.; Shimon, L. J. W.; Milstein, D. PNN Ruthenium Pincer Complexes Based on Phosphinated 2,2′-Dipyridinemethane and 2,2′-Oxobispyridine. Metal−Ligand Cooperation in Cyclometalation and Catalysis. *Organometallics* **2013**, *32*, 2973−2982. (h) Sgro, M. J.; Stephan, D. W. Synthesis and Reactivity of Ruthenium Tridentate Bis-Phosphinite Ligand Complexes. *Dalton Trans.* **2013**, *42*, 10460−72. (i) Balaraman, E.; Srimani, D.; Diskin-Posner, Y.; Milstein, D. Direct Synthesis of Secondary Amines from Alcohols and Ammonia Catalyzed by a Ruthenium Pincer Complex. *Catal. Lett.* **2015**, *145*, 139−144. (j) Chen, T.; Li, H.; Qu, S.; Zheng, B.; He, L.; Lai, Z.; Wang, Z.-X.; Huang, K.-W. Hydrogenation of Esters Catalyzed by Ruthenium PN3-Pincer Complexes Containing an Aminophosphine Arm. *Organometallics* **2014**, *33*, 4152−4155. (k) Fogler, E.; Garg, J. A.; Hu, P.; Leitus, G.; Shimon, L. J. W.; Milstein, D. System with Potential Dual Modes of Metal−Ligand Cooperation: Highly Catalytically Active Pyridine-Based PNNH−Ru Pincer Complexes. *Chem. - Eur. J.* **2014**, *20*, 15727−15731. (l) Ramaraj, A.; Nethaji, M.; Jagirdar, B. R. Contrasting Reactivity Behaviour of the [RuHCl(CO)(PNP)] Complex with Electrophilic Reagents XOTf (X = H, CH_3, Me_3Si). *Dalton Trans.* **2014**, *43*, 14625−35. (m) Tanabe, Y.;

DOI: 10.1021/acs.organomet.8b00470
Organometallics 2018, 37, 3286−3297

Kuriyama, S.; Arashiba, K.; Nakajima, K.; Nishibayashi, Y. Synthesis and Reactivity of Ruthenium Complexes Bearing Arsenic-Containing Arsenic-Nitrogen-Arsenic-Type Pincer Ligand. *Organometallics* **2014**, *33*, 5295−5300. (n) Ye, X.; Plessow, P. N.; Brinks, M. K.; Schelwies, M.; Schaub, T.; Rominger, F.; Paciello, R.; Limbach, M.; Hofmann, P. Alcohol Amination with Ammonia Catalyzed by an Acridine-Based Ruthenium Pincer Complex: A Mechanistic Study. *J. Am. Chem. Soc.* **2014**, *136*, 5923−5929. (o) Hernández-Juárez, M.; López-Serrano, J.; Lara, P.; Morales-Cerón, J. P.; Vaquero, M.; Álvarez, E.; Salazar, V.; Suárez, A. Ruthenium(II) Complexes Containing Lutidine-Derived Pincer CNC Ligands: Synthesis, Structure, and Catalytic Hydrogenation of C-N Bonds. *Chem. - Eur. J.* **2015**, *21*, 7540−55. (p) Xu, Y.; Rettenmeier, C. A.; Plundrich, G. T.; Wadepohl, H.; Enders, M.; Gade, L. H. Borane-Bridged Ruthenium Complex Bearing a PNP Ligand: Synthesis and Structural Characterization. *Organometallics* **2015**, *34*, 5113−5118. (q) Zhang, L.; Han, Z.; Zhao, X.; Wang, Z.; Ding, K. Highly Efficient Ruthenium-Catalyzed N-Formylation of Amines with H_2 and Co_2. *Angew. Chem., Int. Ed.* **2015**, *54*, 6186−9. (r) Alberico, E.; Lennox, A. J.; Vogt, L. K.; Jiao, H.; Baumann, W.; Drexler, H. J.; Nielsen, M.; Spannenberg, A.; Checinski, M. P.; Junge, H.; Beller, M. Unravelling the Mechanism of Basic Aqueous Methanol Dehydrogenation Catalyzed by Ru-PNP Pincer Complexes. *J. Am. Chem. Soc.* **2016**, *138*, 14890−14904. (s) Cabrero-Antonino, J. R.; Alberico, E.; Drexler, H.-J.; Baumann, W.; Junge, K.; Junge, H.; Beller, M. Efficient Base-Free Hydrogenation of Amides to Alcohols and Amines Catalyzed by Well-Defined Pincer Imidazolyl−Ruthenium Complexes. *ACS Catal.* **2016**, *6*, 47−54. (t) Zhang, L.; Nguyen, D. H.; Raffa, G.; Trivelli, X.; Capet, F.; Desset, S.; Paul, S.; Dumeignil, F.; Gauvin, R. M. Catalytic Conversion of Alcohols into Carboxylic Acid Salts in Water: Scope, Recycling, and Mechanistic Insights. *ChemSusChem* **2016**, *9*, 1413−23. (u) Chai, H.; Wang, L.; Liu, T.; Yu, Z. A Versatile Ru(II)-NNP Complex Catalyst for the Synthesis of Multisubstituted Pyrroles and Pyridines. *Organometallics* **2017**, *36*, 4936−4942.

(13) (a) Gunanathan, C.; Ben-David, Y.; Milstein, D. Direct Synthesis of Amides from Alcohols and Amines with Liberation of H_2. *Science* **2007**, *317*, 790−792. (b) Cantillo, D. Mechanistic Insights on the Ruthenium-Catalyzed Hydrogenation of Amides - C-N vs. C-O Cleavage. *Eur. J. Inorg. Chem.* **2011**, *2011*, 3008−3013. (c) Li, H.; Wang, X.; Huang, F.; Lu, G.; Jiang, J.; Wang, Z.-X. Computational Study on the Catalytic Role of Pincer Ruthenium(II)-PNN Complex in Directly Synthesizing Amide from Alcohol and Amine: The Origin of Selectivity of Amide over Ester and Imine. *Organometallics* **2011**, *30*, 5233−5247.

(14) (a) Werkmeister, S.; Junge, K.; Wendt, B.; Alberico, E.; Jiao, H.; Baumann, W.; Junge, H.; Gallou, F.; Beller, M. Hydrogenation of Esters to Alcohols with a Well-Defined Iron Complex. *Angew. Chem., Int. Ed.* **2014**, *53*, 8722−8726. (b) Junge, K.; Wendt, B.; Jiao, H.; Beller, M. Iridium-Catalyzed Hydrogenation of Carboxylic Acid Esters. *ChemCatChem* **2014**, *6*, 2810−2814. (c) Junge, K.; Wendt, B.; Westerhaus, F. A.; Spannenberg, A.; Jiao, H.; Beller, M. Phosphine-Imidazolyl Ligands for the Efficient Ruthenium-Catalyzed Hydrogenation of Carboxylic Esters. *Chem. - Eur. J.* **2012**, *18*, 9011−9018. (d) Ito, M.; Ootsuka, T.; Watari, R.; Shiibashi, A.; Himizu, A.; Ikariya, T. Catalytic Hydrogenation of Carboxamides and Esters by Well-Defined Cp*Ru Complexes Bearing a Protic Amine Ligand. *J. Am. Chem. Soc.* **2011**, *133*, 4240−4242.

(15) (a) Stanton, M. G.; Gagné, M. R. The Remarkable Catalytic Activity of Alkali-Metal Alkoxide Clusters in the Ester Interchange Reaction. *J. Am. Chem. Soc.* **1997**, *119*, 5075−5076. (b) Stanton, M. G.; Allen, C. B.; Kissling, R. M.; Lincoln, A. L.; Gagné, M. R. "New" Catalysts for the Ester-Interchange Reaction: The Role of Alkali-Metal Alkoxide Clusters in Achieving Unprecedented Reaction Rates. *J. Am. Chem. Soc.* **1998**, *120*, 5981−5989.

(16) vom Stein, T.; Meuresch, M.; Limper, D.; Schmitz, M.; Holscher, M.; Coetzee, J.; Cole-Hamilton, D. J.; Klankermayer, J.; Leitner, W. Highly Versatile Catalytic Hydrogenation of Carboxylic and Carbonic Acid Derivatives Using a Ru-Triphos Complex: Molecular Control over Selectivity and Substrate Scope. *J. Am. Chem. Soc.* **2014**, *136*, 13217−13225.

(17) (a) John, J. M.; Bergens, S. H. A Highly Active Catalyst for the Hydrogenation of Amides to Alcohols and Amines. *Angew. Chem., Int. Ed.* **2011**, *50*, 10377−10380. (b) Coetzee, J.; Dodds, D. L.; Klankermayer, J.; Brosinski, S.; Leitner, W.; Slawin, A. M.; Cole-Hamilton, D. J. Homogeneous Catalytic Hydrogenation of Amides to Amines. *Chem. - Eur. J.* **2013**, *19*, 11039−11050. (c) Kita, Y.; Higuchi, T.; Mashima, K. Hydrogenation of Amides Catalyzed by a Combined Catalytic System of a Ru Complex with a Zinc Salt. *Chem. Commun.* **2014**, *50*, 11211−11213. (d) Hu, P.; Ben-David, Y.; Milstein, D. Rechargeable Hydrogen Storage System Based on the Dehydrogenative Coupling of Ethylenediamine with Ethanol. *Angew. Chem., Int. Ed.* **2016**, *55*, 1061−1064. (e) Rezayee, N. M.; Samblanet, D. C.; Sanford, M. S. Iron-Catalyzed Hydrogenation of Amides to Alcohols and Amines. *ACS Catal.* **2016**, *6*, 6377−6383. (f) Schneck, F.; Assmann, M.; Balmer, M.; Harms, K.; Langer, R. Selective Hydrogenation of Amides to Amines and Alcohols Catalyzed by Improved Iron Pincer Complexes. *Organometallics* **2016**, *35*, 1931−1943. (g) Yuan, M.-L.; Xie, J.-H.; Zhu, S.-F.; Zhou, Q.-L. Deoxygenative Hydrogenation of Amides Catalyzed by a Well-Defined Iridium Pincer Complex. *ACS Catal.* **2016**, *6*, 3665−3669. (h) Jayarathne, U.; Zhang, Y.; Hazari, N.; Bernskoetter, W. H. Selective Iron-Catalyzed Deaminative Hydrogenation of Amides. *Organometallics* **2017**, *36*, 409−416. (i) Rasu, L.; John, J. M.; Stephenson, E.; Endean, R.; Kalapugama, S.; Clement, R.; Bergens, S. H. Highly Enantioselective Hydrogenation of Amides Via Dynamic Kinetic Resolution under Low Pressure and Room Temperature. *J. Am. Chem. Soc.* **2017**, *139*, 3065−3071. (j) Shi, L.; Tan, X.; Long, J.; Xiong, X.; Yang, S.; Xue, P.; Lv, H.; Zhang, X. Direct Catalytic Hydrogenation of Simple Amides: A Highly Efficient Approach from Amides to Amines and Alcohols. *Chem. - Eur. J.* **2017**, *23*, 546−548.

(18) (a) Werkmeister, S.; Junge, K.; Wendt, B.; Spannenberg, A.; Jiao, H.; Bornschein, C.; Beller, M. Ruthenium/Imidazolylphosphine Catalysis: Hydrogenation of Aliphatic and Aromatic Nitriles to Form Amines. *Chem. - Eur. J.* **2014**, *20*, 4227−31. (b) Choi, J.-H.; Prechtl, M. H. G. Tuneable Hydrogenation of Nitriles into Imines or Amines with a Ruthenium Pincer Complex under Mild Conditions. *ChemCatChem* **2015**, *7*, 1023−1028. (c) Mukherjee, A.; Srimani, D.; Chakraborty, S.; Ben-David, Y.; Milstein, D. Selective Hydrogenation of Nitriles to Primary Amines Catalyzed by a Cobalt Pincer Complex. *J. Am. Chem. Soc.* **2015**, *137*, 8888−91. (d) Neumann, J.; Bornschein, C.; Jiao, H.; Junge, K.; Beller, M. Hydrogenation of Aliphatic and Aromatic Nitriles Using a Defined Ruthenium PNP Pincer Catalyst. *Eur. J. Org. Chem.* **2015**, *2015*, 5944−5948. (e) Chakraborty, S.; Leitus, G.; Milstein, D. Selective Hydrogenation of Nitriles to Primary Amines Catalyzed by a Novel Iron Complex. *Chem. Commun.* **2016**, *52*, 1812−5. (f) Sato, Y.; Kayaki, Y.; Ikariya, T. Cationic Iridium and Rhodium Complexes with C−N Chelating Primary Benzylic Amine Ligands as Potent Catalysts for Hydrogenation of Unsaturated Carbon−Nitrogen Bonds. *Organometallics* **2016**, *35*, 1257−1264. (g) Adam, R.; Bheeter, C. B.; Cabrero-Antonino, J. R.; Junge, K.; Jackstell, R.; Beller, M. Selective Hydrogenation of Nitriles to Primary Amines by Using a Cobalt Phosphine Catalyst. *ChemSusChem* **2017**, *10*, 842−846. (h) Chakraborty, S.; Milstein, D. Selective Hydrogenation of Nitriles to Secondary Imines Catalyzed by an Iron Pincer Complex. *ACS Catal.* **2017**, *7*, 3968−3972. (i) Mukherjee, A.; Srimani, D.; Ben-David, Y.; Milstein, D. Low-Pressure Hydrogenation of Nitriles to Primary Amines Catalyzed by Ruthenium Pincer Complexes. Scope and Mechanism. *ChemCatChem* **2017**, *9*, 559−563. (j) Tokmic, K.; Jackson, B. J.; Salazar, A.; Woods, T. J.; Fout, A. R. Cobalt-Catalyzed and Lewis Acid-Assisted Nitrile Hydrogenation to Primary Amines: A Combined Effort. *J. Am. Chem. Soc.* **2017**, *139*, 13554−13561.

(19) (a) Fuentes, J. A.; Smith, S. M.; Scharbert, M. T.; Carpenter, I.; Cordes, D. B.; Slawin, A. M. Z.; Clarke, M. L. On the Functional Group Tolerance of Ester Hydrogenation and Polyester Depolymerisation Catalysed by Ruthenium Complexes of Tridentate Aminophosphine Ligands. *Chem. - Eur. J.* **2015**, *21*, 10851−10860. (b) van

DOI: 10.1021/acs.organomet.8b00470
Organometallics 2018, 37, 3286−3297

Putten, R.; Uslamin, E. A.; Garbe, M.; Liu, C.; Gonzalez-de-Castro, A.; Lutz, M.; Junge, K.; Hensen, E. J. M.; Beller, M.; Lefort, L.; Pidko, E. A. Non-Pincer-Type Manganese Complexes as Efficient Catalysts for the Hydrogenation of Esters. *Angew. Chem., Int. Ed.* **2017**, *56*, 7531−7534. (c) Yang, X. H.; Yue, H. T.; Yu, N.; Li, Y. P.; Xie, J. H.; Zhou, Q. L. Iridium-Catalyzed Asymmetric Hydrogenation of Racemic Alpha-Substituted Lactones to Chiral Diols. *Chem. Sci.* **2017**, *8*, 1811−1814.

(20) Ahmad, N.; Levison, J. J.; Robinson, S. D.; Uttley, M. F.; Wonchoba, E. R.; Parshall, G. W. Complexes of Ruthenium, Osmium, Rhodium, and Iridium Containing Hydride Carbonyl, or Nitrosyl Ligands. *Inorg. Synth* **2007**, *15*, 45−64.

(21) Kottas, G.; Xia, C.; Elshenawy, Z.; Ansari, N. Phosphorescent Heteroleptic Phenylbenzimidazole Dopants. U.S. Patent Application 20120292600, Nov 22, 2012.

DOI: 10.1021/acs.organomet.8b00470
Organometallics 2018, 37, 3286−3297